

CHARACTERIZATION OF A YEAST DILUTION PRONGING
ASSAY WITH EPITHELIAL SODIUM CHANNELS
EXPRESSED AS HOMOTRIMERIC α ENAC

Presented to the Graduate Council of
Texas State University-San Marcos
in Partial Fulfillment
of the Requirements

for the Degree

Master of SCIENCE

By

Samantha R. Swann, B.S, B.A.

San Marcos, Texas
May 2013

CHARACTERIZATION OF A YEAST DILUTION PRONGING
ASSAY WITH EPITHELIAL SODIUM CHANNELS
EXPRESSED AS HOMOTRIMERIC α ENAC

Committee Members Approved:

Rachell Booth, Chair

Steve Whitten

Kevin Lewis

Approved:

J. Michael Willoughby
Dean of the Graduate College

COPYRIGHT

by

Samantha R. Swann

2013

FAIR USE AND AUTHOR'S PERMISSION STATEMENT

Fair Use

This work is protected by the Copyright Laws of the United States (Public Law 94- 553, section 107). Consistent with fair use as defined in the Copyright Laws, brief quotations of this material are allowed with proper acknowledgement. Use of this material for financial gain without the author's express written permission is not allowed

Duplication Permission

As the copyright holder of this work I, Samantha R. Swann, refuse permission to copy in excess of the "Fair Use" exemption without my written permission.

ACKNOWLEDGEMENTS

First and foremost, I would like to thank my research advisor Dr. Rachell Booth. There are very few people who find a career that allows them to truly change the lives of others. While many teachers can teach, very few can inspire. She is extremely gifted and I, along with many other of her students, have been privileged to be under her instruction. I was first introduced to biochemistry in her class in the fall of 2009 and specifically pursued this graduate degree because of her inspiration. I want to thank her for all her patience and understanding over the last two years. Her class changed the direction of my life and her teachings as an advisor will remain with me throughout my career.

I would also like to thank my coworkers in this program who have been a fundamental component of my success, Katelyn Ryder and Esther Lee. They are two of the most kind and intelligent people I have ever met. I also feel fortunate to have met my best friend, David Anguiano, during this program. Words cannot describe how much I admire his intelligence and passion for learning. Ty Whisenant and Daniel Horn are two people who I looked to for advice and laughter as I moved through the challenges of my project. I cannot thank all of these individuals enough for their help and motivation over the course of this program. Their friendships, like my degree, I will value for years to come.

Finally, I would like to thank my friends and family for all their support and patience. Without them, I would not be where I am today. Thank you for always encouraging my love for education and helping me fulfill my dreams.

This manuscript was submitted on December 31, 2012.

TABLE OF CONTENTS

| | Page |
|---|-------------|
| ACKNOWLEDGEMENTS | v |
| LIST OF TABLES | viii |
| LIST OF FIGURES | ix |
| CHAPTER | |
| I. INTRODUCTION AND LITERATURE REVIEW | 1 |
| II. MATERIALS AND METHODS | 14 |
| III. RESEARCH RESULTS AND DISCUSSION | 21 |
| IV. CONCLUSIONS | 47 |
| REFERENCES | 49 |

LIST OF TABLES

| Table | Page |
|---|-------------|
| 1: Recipes for 2% glucose or galactose selective plates with 0.5 M salt..... | 19 |
| 2: Recipes for 2% glucose or galactose selective plates with 0.25 M salt..... | 20 |

LIST OF FIGURES

| Figure | Page |
|---|------|
| 1: Translation of genetic conservation within ENaC/Degenerin superfamily | 3 |
| 2: The proposed stoichiometry of α , β , and γ subunits in ENaC | 4 |
| 3: ENaC hormone regulation | 6 |
| 4: Proposed structural model of heterotrimeric $\alpha\beta\gamma$ ENaC..... | 11 |
| 5: Dilution survival pronging assay | 12 |
| 6: Vector map of pYES/NT/A | 22 |
| 7: Gel electrophoresis of pYES2/NT/ α ENaC | 23 |
| 8: Transfection of pYES2/NT/ α ENaC into <i>S. cerevisiae</i> | 24 |
| 9: Patch plate of transfection..... | 25 |
| 10: Control prongings without additional NaCl..... | 27 |
| 11: Standard NaCl control prongings | 28 |
| 12: Competitive sodium inhibition with Li^+ | 30 |
| 13: Prongings of NH_4^+ ions effect on ENaC..... | 32 |
| 14: Prongings of K^+ ions effect on ENaC..... | 34 |
| 15: Prongings of direct sodium self-inhibition by Cl^- ions | 36 |
| 16: Pronging analysis of sodium self-inhibition from Cl^- ions with excess Na^+ ions..... | 37 |
| 17: Pronging analysis at various pH levels with additional 0.25 M NaCl..... | 39 |
| 18: Pronging analysis at various pH levels with additional 0.5 M NaCl..... | 40 |
| 19: Ion regulation of ENaC at 16 °C and 37 °C on 2% galactose..... | 43 |

20: Ion regulation of ENaC at 16 °C and 37 °C on 2% glucose.....44

CHAPTER I

INTRODUCTION AND LITERATURE REVIEW

Membrane ion channels play a pivotal role in the regulation of homeostasis within the body. Physiological function relies on the cell's ability to transport important information or materials from the extracellular medium across the cell membrane. Ion channels facilitate this process as they selectively allow passage in accordance with the cell gradient. This is seen in the epithelial sodium channel (ENaC), one of the most selective ion channels, specific for Na⁺ ions but permeable to Li⁺ ions and protons. ENaC can be found in the glucocorticoid responsive epithelia of the alveolar tissue, the aldosterone responsive epithelia of the distal colon, and collecting tubules of the kidney (1,2). Within the lungs, ENaC is responsible for fluid reabsorption after birth as the lungs transition from fluid to air intake. In the colon and collecting tubules of the kidney, the primary function of ENaC is to regulate blood pressure and fluid balance.

Within the kidney there are close to a million functional units termed nephrons that are filtering the blood to remove waste. The functional unit is made up of a glomerulus, proximal tubule, collecting duct, and distal tubule. As urine passes through the apical side of the epithelia to be excreted for waste, the vast majority of sodium is reabsorbed in the proximal tubules. According to physiological need, the collecting ducts

then reabsorb water, concentrating the ions remaining. Ultimately, the last few percent of sodium ions are reabsorbed through ENaC in the distal tubules. Although numerically small, this final step in reabsorption of sodium ions from the extracellular fluid is critical in maintaining water and electrolyte balance. Sodium concentration in the epithelial cell is maintained by the sodium/potassium pump located on the basolateral side of the cell. Passage is permitted against the concentration gradient with energy obtained from the dephosphorylation of adenosine triphosphate (ATP). Sodium ions are then absorbed into the blood stream through the peritubular capillaries of the kidney. To regulate ion concentration in the blood, water is readily absorbed in conjunction with sodium through separate aquaporins also in the epithelia. As ion and water concentration increase in blood circulation, the arterial system experiences an increase in overall volume, forcing the heart to work harder to circulate blood. This increase in blood pressure leads to a clinical state of hypertension, a precursor to multiple diseases including heart disease, the leading cause of mortality in the U.S. (3).

ENaC is a member of the ENaC/Degenerin superfamily of cation channels, a group of transmembrane ion proteins that function specifically in sodium absorption (4,5). Other members of this family include the acid-sensing ion channel (ASIC), the ripped pocket/picked pocket channel, and the degenerin (5). ASIC functions in sensory neurons and is ligand gated by protons that, in excess, create an acid environment outside the cell (5,6). The ripped pocket/picked pocket channel has been found to function in *Drosophila* larva through transduction of mechanical stimuli from heat (5). Degenerins are found in *C. elegans*, a species of worm that uses sodium reabsorption to facilitate transduction of mechanical stimuli from touch (5). The classification of these proteins

into this family is due to topological similarities that stem from genetic conservation between each member (Figure 1).

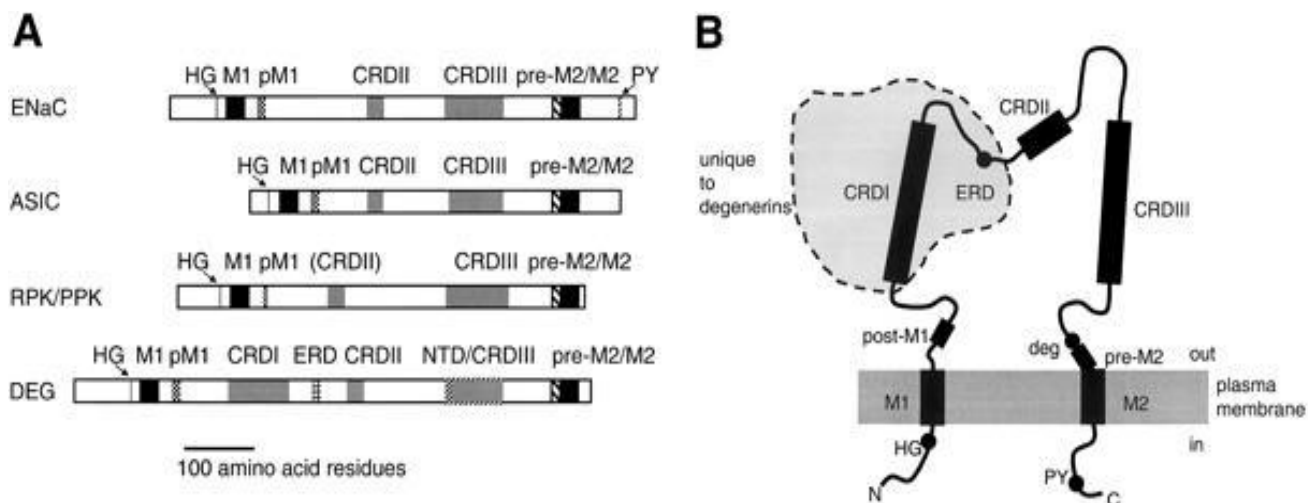


Figure 1. Translation of genetic conservation within ENaC/Degenerin superfamily (7).

These genes ultimately all code for the evolved structure of two transmembrane alpha helices connected by a highly conserved cysteine-rich extracellular loop and short N- and C- termini in the cytoplasm (7). Unique to degenerins is a second cysteine-rich region (CDR1) within the extracellular loop and an extracellular regulating domain (ERD), leaving ENaC to be most structurally similar to the acid-sensing ion channel and the ripped pocket/picked pocket channels. Another unique feature shared in this family is the conserved genes that code for an amino acid sequence with high affinity for amiloride binding. For all members of the family, amiloride competes with sodium to block the pore region of the channel, but increased affinity is seen for ENaC. This increased sensitivity is due to the unique presence of the amino acid serine in comparison to glycine as seen in the other three family members (8).

The structure of ENaC is the foundation of its ability to function properly. Three subunits termed α , β , and γ make up the complex, and are likely heterotrimeric (Figure 2) (9).

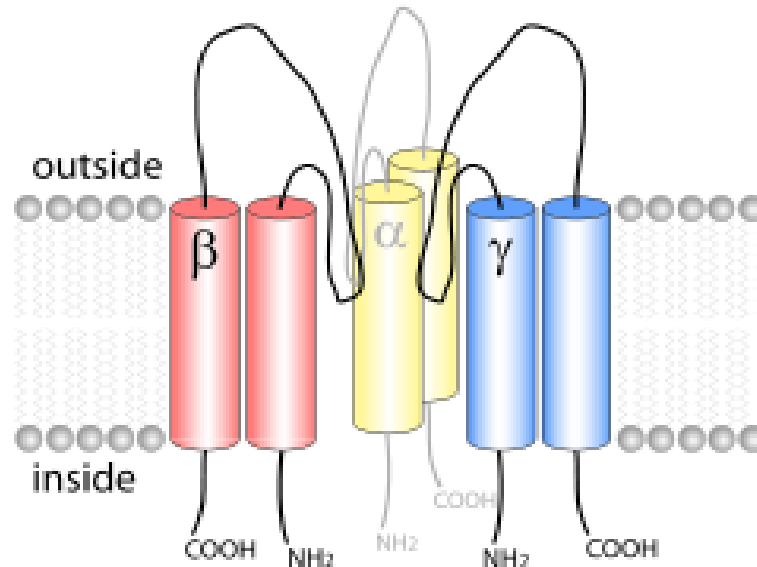


Figure 2. The proposed stoichiometry of α , β , and γ subunits in the ENaC integral protein (9)

The three subunits contain 698(α), 638(β), and 650(γ) amino acids and are homologous in sequence and topology (10). On a genomic level, all three $\alpha\beta\gamma$ subunits are coded for on individual genes, SCNN1A, SCNN1B, and SCNN1G, respectively. However, the SCNN1A gene for the α subunit is located on a separate chromosome than the β and γ genes which are found in close range to one another on the same chromosome (11). The α subunit can function at a basal level independently of the β and γ subunits, but expression studies show an increased potentiation of channel function when all three are combined and allowed to work synergistically (12). Unlike the α subunit, the β and γ subunits cannot function individually or together, indicating that the α subunit could be

primarily responsible for the function of the ion selective pore, although all three subunits contribute to its formation (9).

Within the luminal membrane of the epithelial cells, ENaC is constitutively active and sodium absorption is largely dictated by the numerical amount of ENaCs present. However, the configuration of the heteromeric protein provides a structural limitation to the rate of sodium absorption into the cell (13). The biological necessity for ion absorption has created selective pressure for the expression of various configurations of $\alpha\beta$, $\alpha\gamma$, and α alone. Each configuration has unique properties that structurally lead to changes in pore size and rate of ion reabsorption (13). Within the nephron, 95% of sodium reabsorption has already taken place in the proximal tubules, requiring an efficient absorption of the remaining sodium in the distal tubules to maintain fluid homeostasis. To accomplish this, ENaC is configured as heterotrimeric $\alpha\beta\gamma$ in distal tubule epithelia, providing an increased rate of sodium absorption (13).

The numeric amount of ENaCs in the membrane is the ultimate determinant of sodium absorption activity. As shown in Figure 3, the regulation of ENaC apical insertion and degradation is controlled by the stimulated release of aldosterone, vasopressin, and ubiquitination by NEDD4.

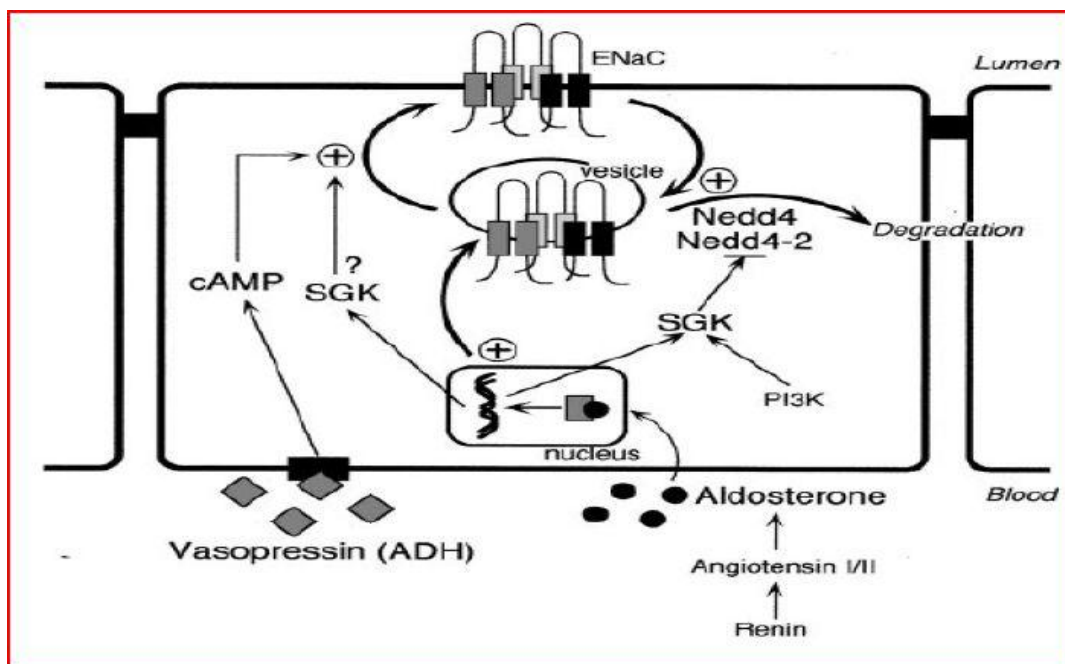


Figure 3. ENaC hormone regulation. Schematic overview of aldosterone stimulation of α ENaC transcription, vasopressin stimulation of vesicle ENaC exocytosis from ER, and indirect down-regulation of ENaC through NEDD4 affiliated ubiquitination (14).

In physiological states of low blood pressure and low sodium, the granular cells of the nephron initiate the stimulated the release of aldosterone, the final product of the renin-angiotensin cascade. Aldosterone binds to steroid receptors and upon infusion into the cell, signals for an early (1-3 h) and late phase (6-24 h) response (14). The early stage is characterized by an increase in the transcription of genes that modulate the trafficking and activity of ENaC, such as serum/gluocorticoid regulated kinase (SGK). It is hypothesized that either ENaC is directly phosphorylated at the C- terminus of the β or γ subunit or other intermediate proteins that control expression of ENaC are phosphorylated. The consistent outcome is that SGK is stimulated by aldosterone to increase the amount of ENaC at the cell surface (14,15). There is also an indirect method of increased regulation from SGK through the inhibition of NEDD4 modulated ubiquitination. This occurs as SGK recognizes and binds to the PY motif of NEDD4-2,

resulting in phosphorylation of the protein that prevents binding to ENaC (14, 16, 17). This allows for the numeric amount of ENaCs to consistently increase without removal, allowing for greater sodium influx into the cell.

The late phase of aldosterone stimulation occurs through increased transcription of the alpha subunit gene, the functional determinant of the protein complex (14, 15). The β and γ subunit expression are not stimulated by aldosterone in the tissue of the kidney distal tubules. However, there is an aldosterone stimulated proteolytic cleavage of a 70 kDa fragment on the C- terminus of γ ENaC that is thought to be mediated through the serine protease CAP1 (14). Through possible increase in stabilization of α ENaC mRNA or protein, the rate limiting step for ENaC expression is accomplished with the translation of the α ENaC subunit. Within the endoplasmic reticulum (ER), the β and γ ENaC subunits have already been translated and can complex with the new α ENaC to form a functional heteromeric protein (18). Ultimately all three subunits are inserted into the luminal membrane of the cell, but whether the quaternary structure takes form in the secretory vesicle leaving the ER or once the individual subunits are placed in the membrane is still unclear.

In correlation with aldosterone, vasopressin also plays a role in the increased expression of ENaC at the cell membrane. In response to osmotic changes, the hypothalamus releases vasopressin which binds to V2 receptors alongside the basolateral membrane (14). As seen in Figure 3, this binding activates adenylate cyclase which increases the production of cAMP. As cellular concentrations of cAMP rise, the exocytosis of ENaC from the vesicle pool of the ER is stimulated, assisting in the up-regulation and increase of numeric channel complexes at the cell membrane (14).

The down regulation of ENaC is modulated by NEDD4, a small regulatory protein that is a member of the ubiquitin ligase family. The binding of NEDD4 to the PY motifs of the C-terminus of α , β , or γ subunits signals the protein for ubiquitination (14, 19, 20). This is a two-step reaction that is enzymatically accomplished with the dephosphorylation of ATP (14). Ultimately, polyubiquitination results in proteasome recognition and degradation of the protein from the cell membrane. This removal of ENaC results in a decrease in numeric proteins at the cell surface, impairing sodium influx into the cell.

As is common in distal targets of hormone regulated proteins, the time lapse for complete response can range from minutes to hours. Investigation into the possible fine-tuning of the channel via monovalent and divalent cations was stimulated by the functional similarities seen between members of the ENaC/Degenerin superfamily, all of which contain extracellular loops that contribute to some form of vital regulation in protein activity (21). Upon investigation, Garty identified the occurrence of extracellular sodium self-inhibition, a phenomenon that likely occurs to prevent detrimental changes in intracellular concentration in the event of rapid sodium increase in physiological conditions (22, 23). Further patch clamping studies have shown a self-inhibitory effect of ENaC in the presence of Na^+ , Cl^- and variations in pH. Evidence for this extracellular regulation is seen in studies from Sheng and associates as they identified mutations of His²³⁹ γ ENaC and His²⁸² α ENaC to respectively prevent and enhance sodium self-inhibition as corresponding changes in single channel conductance of sodium passage were observed (24). Cl^- ions have shown two inhibitory methods: indirectly, through the promotion of Na^+ self-inhibition and directly, though plausible interactions between

subunit binding domains (25). The crystal structure of ASIC shows desensitization to Na^+ passage in the presence of excess Cl^- due to these same mechanisms of inhibition. With evidence of structural homology between ASIC and ENaC, Collier and Snyder identified two homologous residues, $\alpha\text{ENaC His}^{418}$ and $\beta\text{ENaC Arg}^{388}$, that upon mutation, remove inhibitory effects of Cl^- (25). Collier and Snyder also used patch clamping to investigate how physiological range of pH from 6.5 to 8.5 effects sodium influx. They found that in human ENaC H441 epithelia, acidic pH levels were associated with an increase in sodium current, but more alkaline levels possibly induced a decrease in sodium current (26). It is hypothesized that proton concentration alters sodium self-inhibition. To further this study, both colleagues found that mutations altering sodium self-inhibition showed corresponding alterations with pH adjustments. Although it has not been studied, NH_4^+ is also found in the urine in response to acidosis and could also play a role in minimizing sodium self-inhibition in correlation with low pH levels. Another ion that has not yet been investigated to play a role in sodium self-inhibition is K^+ , which is inversely related to Na^+ influx within the epithelial cell. High intracellular K^+ corresponds with low intracellular Na^+ levels as three Na^+ for every two K^+ is inversely exchanged at the basolateral membrane. As K^+ increases in the extracellular lumen from passage via intracellular potassium pumps, concentration levels outside the cell might modulate ENaC to increase sodium influx to raise depleting intracellular concentrations. These various studies and speculations have led to the belief in the existence of a possible allosteric site that might be responsible for changes to pore diameter, minimizing or maximizing rapid influx of sodium into the cell.

Malfunction of this membrane ion channel can lead to salt sensitive hypertension and possible detrimental effects as seen in Liddle's syndrome and pseudohypoaldosteronism type 1 (PHA-1) (1). These inherited monogenetic disorders are a result of a point or frameshift mutation and cause functional or structural malfunction to the ENaC protein (1). Liddle's syndrome is an autosomal dominant disorder that causes hyperactivity of ENaC due to a mutation to the C-terminus of the β or γ subunit that results in the loss of up to 75 amino acids (1). This change to the PY motif prevents binding to the ubiquitin ligase protein, NEDD4 which is responsible for degrading the protein to inactivate function (14). Without this repression, the increase of ENaC activity leads to severe hypertension among many other related symptoms. PHA-1 affects ENaC differently depending on whether its onset is from the autosomal dominant or recessive form. These inherited disorders cause hypoactivity through mutations to the mineralocorticoid receptor gene or to the genes encoding subunits of ENaC respectively (1). The decrease or loss of function in ENaC results in severe neonatal salt wasting and hypotension that is non-responsive to mineralocorticoid treatment (1).

Despite progress in the understanding of ENaC and its biological importance, the exact stoichiometry of the protein structure has yet to be confirmed, leaving treatment and possible genetic restoration of diseases associated with ENaC to remain elusive. The acid-sensing ion channel 1 (ASIC1) has recently been confirmed by x-ray crystallization studies as homotrimeric, leading to the plausibility that the ENaC protein could function similarly (27). Stockand and associates have used the crystal structure of ASIC to align homologous segments of ENaC amino acid sequences, creating a proposed structure of ENaC in $\alpha\beta\gamma$ heterotrimeric configuration. (Figure 4) (9).

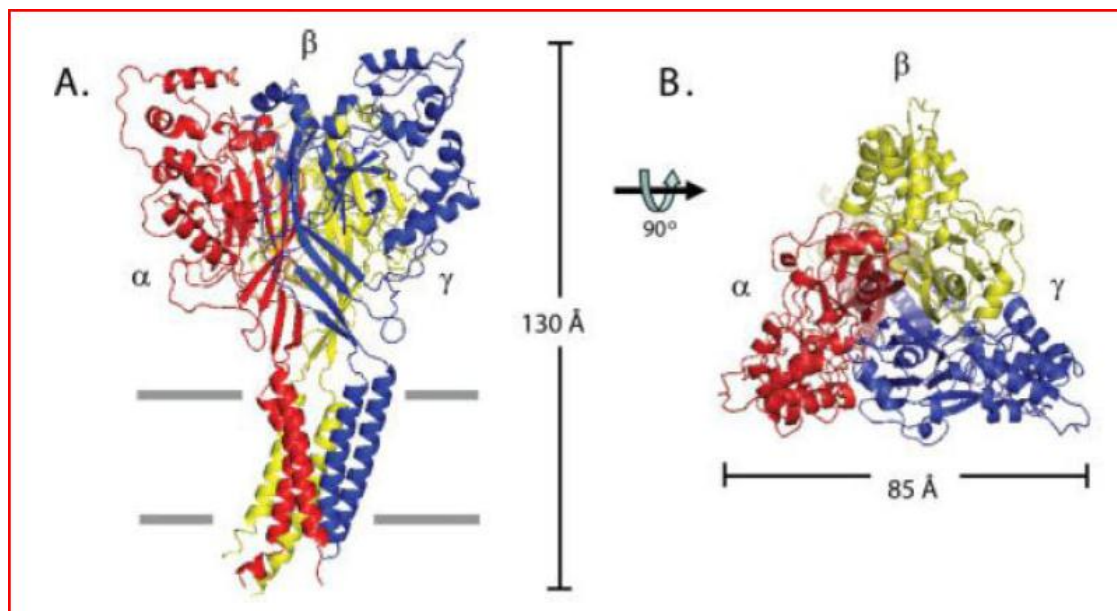


Figure 4. Proposed structural model of heterotrimeric $\alpha\beta\gamma$ ENaC based on homologous acid-sensing ion channel structure determined by x-ray crystallography (9, 27).

In efforts to elucidate the structure of ENaC, genetic mutations have been induced to determine which amino acids are critical to its function and structure. The α subunit operates at a basal level as a homotrimeric protein and therefore can be studied individually (28). Low expression levels of ENaC in mammalian cells have made it challenging to effectively study ENaC in mammalian systems (29). A simplistic and very efficient model organism used in the research of ENaC is the yeast *Saccharomyces cerevisiae*. With this recombinant system, ENaC genes can be expressed from plasmids under the control of strong promoters. Random mutations can be differentiated through a pronging assay that provides a visual phenotype of loss or gain in function of ENaC due to mutation. ENaC in the membrane provides passage of sodium inside the yeast cell, disrupting homeostasis, causing growth inhibition and possible cell death. Recent research conducted by Ty Whisenant (Booth Lab; Texas State University-San Marcos)

has shown yeast sensitivity to salt levels when transformed with a plasmid containing the sequence for the α ENaC subunit (Figure 5).

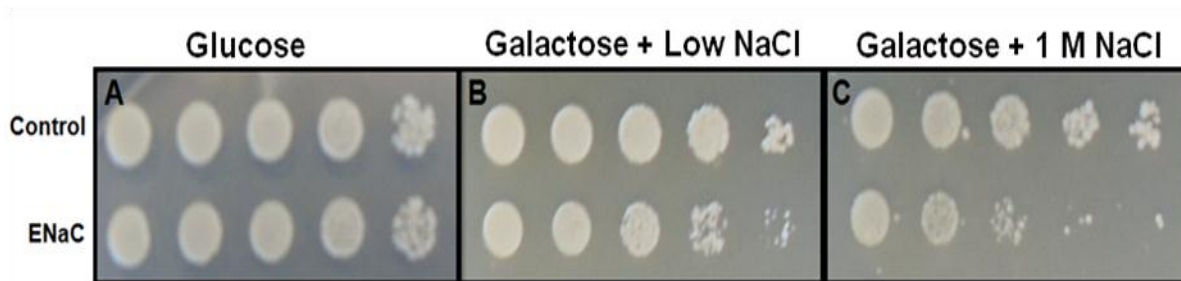


Figure 5. Dilution survival pronging assay of *S. cerevisiae* transfected with functional pYES2/NT/ α ENaC (bottom row) and control pYES2/NT/A (empty vector) (top row).

As mutations were induced along the α sequence, lack of salt sensitivity in the transformed yeast colonies provided a visual screen for genes that contain a critical mutation affecting the function or structure of ENaC. These plasmids were extracted from the yeast cells, transformed back into *E. coli* cells for concentration with cell growth, and then sequenced.

These mutations have been analyzed according to their amino acid location on Stockand's model protein structure of $\alpha\beta\gamma$ ENaC. Mutations close to the pore region were hypothesized to be implicated in function, with mutations along the extracellular loop related to inter/intra subunit binding. However, with speculation of possible allosteric monovalent/divalent cation regulation, a screening mechanism has been created to further analyze the structure-function role these critical mutations might have. The purpose of this thesis project was to first clarify possible changes in yeast growth with homotrimeric α ENaC in the presence of excess Na^+ , Cl^- , K^+ , NH_4^+ , H^+ ions and at growth temperatures

16 °C, 30 °C, and 37 °C. With a standard baseline of ion effects with the functional wildtype complex, critical mutations were screened for the loss/gain of function in ENaC, resulting in increased or decreased yeast growth, respectively. Ultimately, analysis of all three heteromeric combinations $\alpha\alpha\alpha$, $\alpha\beta\beta$, and $\alpha\beta\gamma$ will provide a further insight to which critical amino acids are responsible for interacting with regulatory cations, ions, and protons.

CHAPTER II

MATERIALS AND METHODS

Plasmid Transformation into *E. coli*

Stocks of 100 μ L Top 10 competent *E. coli* cells were mixed with 1-3 μ g pYES2/NT/ α ENaC or pYES2/NT/A (Empty Vector) plasmid DNA that ranged from 0.15-3.0 μ g concentration and set on ice for 20 minutes. The reaction mixture was then heated at 42° C for 45 seconds followed by placement back on ice for 2 minutes. After an addition of 1 mL Luria-Bertani broth, the mixture was incubated at 37° C with shaking at 220 rpm for 1 hour. Upon completion, 50-200 μ L were spread onto LB agar plates made with 40 g/L LB agar miller mix from Genesee Scientific (San Diego, CA) with 100 μ g/mL ampicillin and inverted for growth overnight at 37° C.

Plasmid Isolation from *E. coli*

Top 10 competent *E. coli* cells containing the plasmid DNA was streaked for isolated colonies on LB agar plates with 100 μ g/mL ampicillin and incubated overnight at 37° C. A single colony was utilized to inoculate an overnight culture in 5 mL LB broth with ampicillin and the culture was set to incubate at 37° C with shaking at 220 rpm. Five milliliters of culture were then pelleted and plasmid DNA was isolated according to the

manufacturer's protocol of Qiagen QIAprep Spin Miniprep kit (Valencia, CA). Indicated by manufacturer's instruction were the use of buffers for cell lyses, centrifugation of cellular debris to separate them from supernatant containing nucleic acid, and chromatographic columns for plasmid isolation upon elution with 50 μ L warm water. Concentrations were determined from a 2 μ L drop with a Nanodrop ND-1000 spectrophotometer from Thermo Fisher Scientific (Wilmington, DE). The presence of pYES2/NT/ α ENaC was verified via agarose gel electrophoresis.

Horizontal Gel Electrophoresis

To separate DNA, 0.3-1.9 μ g of samples were loaded into a 1% (w/v) agarose gel made by mixing 50 mL 1X TAE Buffer (40 mM Tris-base, pH 8, 20 mM acetic acid, 1 mM EDTA) and agarose from Shelton Scientific (Shelton, CT). Before the gel was cast, 1 μ g of ethidium bromide solution was added. The gel was placed into a horizontal electrophoresis apparatus from IBI (Peosta, IA), and 1X Tris-acetate-EDTA buffer was added until the gel was fully submerged. A total volume of 6 μ L sample mixture (2-3 μ L sample, 2-3 μ L water, and 1X Promega (Madison, WI) loading dye) was loaded into each well with the same volume of a 1 Kb DNA ladder from New England BioLabs (Beverly, MA). Electrophoresis was conducted for 1 hour at 110 volts. DNA was visualized under UV light in Alpha Innotech Red Gel Imaging System (Santa Clara, CA).

Rapid Transfection into Stationary Phase Yeast Cells

This protocol was a modification from Soni, *et al* (1993). A Beckman Coulter Microfuge 18 centrifuge (Fullerton, CA) at 18,000 g for 30 seconds was utilized

throughout the Rapid Transfection protocol unless otherwise indicated. The yeast strain S1-InsE4A was used for transformation. The genotype of the strain is *MATalpha ura3-52 leu2-3,112 trp1-289 his7-2 ade5-1 lys2::InSE-4A*. An overnight culture was grown in 5 mL YPDA broth (1% w/v yeast extract, 2% w/v peptone, 0.02% adenine, and 2% w/v glucose) at 30° C with shaking at 220 rpm. From that culture, 1 mL of cells was pelleted by centrifugation and the supernatant was removed. Cells were pretreated with 50 µM dithiothreitol for 20 minutes at 42° C. The mixture was then centrifuged and the supernatant removed. The pretreated cells were then mixed with recently boiled sonicated salmon DNA 0.05 mg (Stratagene) and 0.2-3 µg plasmid DNA. After briefly vortexing on a VRW MiniVortexer MV1 (Batavia, IL) at maximum speed, and the cell/DNA sample was mixed with 500 µL of PEG/LiAc/Tris/EDTA solution (0.2 g polyethylene glycol 4000 molecular weight, 5 µM lithium acetate, 0.05 µM EDTA, 5 µM Tris (pH 7.5), 35 µL sterile water). DMSO was added at 1/10th sample volume (approx. 56 µL) and vortexed at maximum speed. The mixture was incubated at room temperature for 15 minutes on a VWR Rocking Platform (Radnor, PA) then transferred to 42° C for an additional 15 minutes. The mixture was centrifuged and the supernatant removed. The pellet was rinsed in 500 µL sterile water without vortexing and then removed from the pellet for disposal. The cells were resuspended in 200 µL sterile water and 10-100 µL was spread onto 2% glucose plates selective for uracil. The plates were incubated at 30° C for 3 days. Single colonies could then be selected to form patch plates for experimental use.

Survival Dilution Pronging Assay

A 2 mm clump of cells was selected from fresh plates of transfected *S. cerevisiae* S1-InsE4A with individual pYES2/NT/ α ENaC and pYES2/NT/A and mixed in 300 μ L sterile water to create assay stock solutions. After vortexing briefly for 5 seconds, a 1/40 dilution of the stock solution was made in 1 mL of sterile water. This solution was also vortexed for 5 seconds and then sonicated with a Sonics Vibracell Ultrasonic Processor (Newtown, CT) between two to three watts for 6-8 seconds. Twelve microliters of the diluted solution was placed into a Reichert hemocytometer (Buffalo, NY) and a cell count was performed under 40X objective using Comcon LOMO phase contrast microscope. Yeast cells at the G₂ stage of growth were counted as a single cell. The cell count was used to calculate the quantity of stock solution necessary to create a 1×10^7 standardized cell dilution in 220 μ L total volume for column one of a 96 well plate. The remaining columns 2-6 were filled with 160 μ L sterile water and a 1:5 dilution was achieved by transferring 40 μ L from each column, starting at the first, to the subsequent column. The pronging apparatus was placed in the 96 well plate and an equal volume of cells were transferred as the apparatus was gently laid on a selective plate containing 2% glucose or galactose with varying salts.

Media Plates

Tables 1 and 2 provide an inclusive list of ingredients utilized to create each plate condition. As indicated, all plates contained either 2% glucose or 2% galactose with 100 μ g/ml ampicillin and were made selective for the *S. cerevisiae* S1-InsE4A yeast strain through the omission of uracil. Control plates consisted of the 2% glucose and 2%

galactose minus ura alone as well as 2% glucose and 2% galactose mixed with individual 0.5 M and 0.25 M NaCl. Alternative salts were added at total concentrations of 0.5 M and 0.25 M alone or in combination with NaCl. Varying amounts of dilute HCl and KOH were utilized to create pH plates. Water volumes were adjusted according to displacement of solid and liquid additives. The plates were grown at either 16° C, 30° C, or 37° C for 2-14 days and imaged with Alpha Innotech Red Gel Imaging System (Santa Clara,CA).

Table 1: Recipes for 2% glucose or galactose selective plates with 0.5 M salt

| TOI | | 0.5M | Drop | | | | | | | | AUTO | AMP | Glu 2% | Gal 2% |
|-----|--|------|-------|-------|------|---------|-------|-------|-------|---|-------|--------------|--------|--------|
| VOL | | NaCl | Out | YNB | Agar | H2O | His | Trp | Leu | SALT 0.5M | CLAVE | 100 mg/mL | 40% | 20% |
| | | | | | | | | | | | | | | |
| | PH | | | | | | | | | HCL/POH | | | | |
| 100 | Glucose | 2.9g | 0.14g | 0.67g | 3.0g | 89.7mL | 0.2mL | 0.5mL | 1.0mL | ?? | | 0.1mL | 5.0mL | |
| 100 | Galactose | 2.9g | 0.14g | 0.67g | 3.0g | 84.7mL | 0.2mL | 0.5mL | 1.0mL | ?? | | 0.1mL | | 10.0mL |
| | | | | | | | | | | | | | | |
| | LiCl | | | | | | | | | LiCl | | | | |
| 100 | Glucose | | 0.14g | 0.67g | 3.0g | 84.75mL | 0.2mL | 0.5mL | 1.0mL | 6.25mL | | 0.1mL | 5.0mL | |
| 100 | Galactose | | 0.14g | 0.67g | 3.0g | 79.75mL | 0.2mL | 0.5mL | 1.0mL | 6.25mL | | 0.1mL | | 10.0mL |
| | | | | | | | | | | | | | | |
| | LiCl | | | | | | | | | LiCl | | | | |
| 100 | Glucose | 2.9g | 0.14g | 0.67g | 3.0g | 82.75mL | 0.2mL | 0.5mL | 1.0mL | 6.25mL | | 0.1mL | 5.0mL | |
| 100 | Galactose | 2.9g | 0.14g | 0.67g | 3.0g | 77.75mL | 0.2mL | 0.5mL | 1.0mL | 6.25mL | | 0.1mL | | 10.0mL |
| | | | | | | | | | | | | | | |
| | KCl | | | | | | | | | KCl | | | | |
| 100 | Glucose | | 0.14g | 0.67g | 3.0g | 89.5mL | 0.2mL | 0.5mL | 1.0mL | 3.728g | | 0.1mL | 5.0mL | |
| 100 | Galactose | | 0.14g | 0.67g | 3.0g | 84.5mL | 0.2mL | 0.5mL | 1.0mL | 3.728g | | 0.1mL | | 10.0mL |
| | | | | | | | | | | | | | | |
| | KCl | | | | | | | | | KCl | | | | |
| 100 | Glucose | 2.9g | 0.14g | 0.67g | 3.0g | 88.2mL | 0.2mL | 0.5mL | 1.0mL | 3.728g | | 0.1mL | 5.0mL | |
| 100 | Galactose | 2.9g | 0.14g | 0.67g | 3.0g | 83.2mL | 0.2mL | 0.5mL | 1.0mL | 3.728g | | 0.1mL | | 10.0mL |
| | | | | | | | | | | | | | | |
| | C₆H₅Na₃O₇·2H₂O | | | | | | | | | 0.167M C ₆ H ₅ Na ₃ O ₇ ·2H ₂ O | | | | |
| 100 | Glucose | | 0.14g | 0.67g | 3.0g | 82.35mL | 0.2mL | 0.5mL | 1.0mL | 14.71g | | 0.1mL | 5.0mL | |
| 100 | Galactose | | 0.14g | 0.67g | 3.0g | 77.35mL | 0.2mL | 0.5mL | 1.0mL | 14.71g | | 0.1mL | | 10.0mL |
| | | | | | | | | | | | | | | |
| | C₆H₅Na₃O₇·2H₂O | | | | | | | | | 0.167M C ₆ H ₅ Na ₃ O ₇ ·2H ₂ O | | | | |
| 100 | Glucose | 2.9g | 0.14g | 0.67g | 3.0g | 81.0mL | 0.2mL | 0.5mL | 1.0mL | 14.71g | | 0.1mL | 5.0mL | |
| 100 | Galactose | 2.9g | 0.14g | 0.67g | 3.0g | 76.0mL | 0.2mL | 0.5mL | 1.0mL | 14.71g | | 0.1mL | | 10.0mL |
| | | | | | | | | | | | | | | |
| | NH₄Cl | | | | | | | | | NH ₄ Cl | | | | |
| 100 | Glucose | | 0.14g | 0.67g | 3.0g | 89.25mL | 0.2mL | 0.5mL | 1.0mL | 2.674g | | 0.1mL | 5.0mL | |
| 100 | Galactose | | 0.14g | 0.67g | 3.0g | 84.25mL | 0.2mL | 0.5mL | 1.0mL | 2.674g | | 0.1mL | | 10.0mL |
| | | | | | | | | | | | | | | |
| | NH₄Cl | | | | | | | | | NH ₄ Cl | | | | |
| 100 | Glucose | 2.9g | 0.14g | 0.67g | 3.0g | 86.35mL | 0.2mL | 0.5mL | 1.0mL | 2.674g | | 0.1mL | 5.0mL | |
| 100 | Galactose | 2.9g | 0.14g | 0.67g | 3.0g | 81.35mL | 0.2mL | 0.5mL | 1.0mL | 2.674g | | 0.1mL | | 10.0mL |

Table 2: Recipes for 2% glucose or galactose selective plates with 0.25 M salt

| TOT VOL | | 0.25M NaCl | Drop Out | YNB | Agar | H ₂ O | His | Trp | Leu | SALT 0.25M | AUTO CLAVE | AMP 100 mg/mL | Glu 2% 40% | Gal 2% 20% |
|---------|--|------------|----------|-------|------|------------------|-------|-------|-------|---|------------|---------------|------------|------------|
| | PH | | | | | | | | | HCL/POH | | | | |
| 100 | Glucose | 1.45g | 0.14g | 0.67g | 3.0g | 90.4mL | 0.2mL | 0.5mL | 1.0mL | ?? | | 0.1mL | 5.0mL | |
| 100 | Galactose | 1.45g | 0.14g | 0.67g | 3.0g | 85.4mL | 0.2mL | 0.5mL | 1.0mL | ?? | | 0.1mL | | 10.0mL |
| | LiCl | | | | | | | | | LiCl | | | | |
| 100 | Glucose | | 0.14g | 0.67g | 3.0g | 87.9mL | 0.2mL | 0.5mL | 1.0mL | 3.125mL | | 0.1mL | 5.0mL | |
| 100 | Galactose | | 0.14g | 0.67g | 3.0g | 82.9mL | 0.2mL | 0.5mL | 1.0mL | 3.125mL | | 0.1mL | | 10.0mL |
| | LiCl | | | | | | | | | LiCl | | | | |
| 100 | Glucose | 1.45g | 0.14g | 0.67g | 3.0g | 83.4mL | 0.2mL | 0.5mL | 1.0mL | 3.125mL | | 0.1mL | 5.0mL | |
| 100 | Galactose | 1.45g | 0.14g | 0.67g | 3.0g | 78.4mL | 0.2mL | 0.5mL | 1.0mL | 3.125mL | | 0.1mL | | 10.0mL |
| | KCl | | | | | | | | | KCl | | | | |
| 100 | Glucose | | 0.14g | 0.67g | 3.0g | 90.3mL | 0.2mL | 0.5mL | 1.0mL | 1.864g | | 0.1mL | 5.0mL | |
| 100 | Galactose | | 0.14g | 0.67g | 3.0g | 85.3mL | 0.2mL | 0.5mL | 1.0mL | 1.864g | | 0.1mL | | 10.0mL |
| | KCl | | | | | | | | | KCl | | | | |
| 100 | Glucose | 1.45g | 0.14g | 0.67g | 3.0g | 89.6mL | 0.2mL | 0.5mL | 1.0mL | 1.864g | | 0.1mL | 5.0mL | |
| 100 | Galactose | 1.45g | 0.14g | 0.67g | 3.0g | 84.6mL | 0.2mL | 0.5mL | 1.0mL | 1.864g | | 0.1mL | | 10.0mL |
| | C₆H₅Na₃O₇·2H₂O | | | | | | | | | 0.0833M C ₆ H ₅ Na ₃ O ₇ ·2H ₂ O | | | | |
| 100 | Glucose | | 0.14g | 0.67g | 3.0g | 83.0mL | 0.2mL | 0.5mL | 1.0mL | 7.9mL | | 0.1mL | 5.0mL | |
| 100 | Galactose | | 0.14g | 0.67g | 3.0g | 78.0mL | 0.2mL | 0.5mL | 1.0mL | 7.9mL | | 0.1mL | | 10.0mL |
| | C₆H₅Na₃O₇·2H₂O | | | | | | | | | 0.0833M C ₆ H ₅ Na ₃ O ₇ ·2H ₂ O | | | | |
| 100 | Glucose | 1.45g | 0.14g | 0.67g | 3.0g | 81.7mL | 0.2mL | 0.5mL | 1.0mL | 7.9mL | | 0.1mL | 5.0mL | |
| 100 | Galactose | 1.45g | 0.14g | 0.67g | 3.0g | 76.7mL | 0.2mL | 0.5mL | 1.0mL | 7.9mL | | 0.1mL | | 10.0mL |
| | NH₄Cl | | | | | | | | | NH ₄ Cl | | | | |
| 100 | Glucose | | 0.14g | 0.67g | 3.0g | 90.13mL | 0.2mL | 0.5mL | 1.0mL | 1.37g | | 0.1mL | 5.0mL | |
| 100 | Galactose | | 0.14g | 0.67g | 3.0g | 85.13mL | 0.2mL | 0.5mL | 1.0mL | 1.37g | | 0.1mL | | 10.0mL |
| | NH₄Cl | | | | | | | | | NH ₄ Cl | | | | |
| 100 | Glucose | 1.45g | 0.14g | 0.67g | 3.0g | 89.46mL | 0.2mL | 0.5mL | 1.0mL | 1.37g | | 0.1mL | 5.0mL | |
| 100 | Galactose | 1.45g | 0.14g | 0.67g | 3.0g | 84.46mL | 0.2mL | 0.5mL | 1.0mL | 1.37g | | 0.1mL | | 10.0mL |

CHAPTER III

RESULTS AND DISCUSSION

The goal of this research was to use the yeast screen, but evaluate growth in the presence of excess monovalent and divalent cations within the media. Critical mutations have been identified using homotrimeric α ENaC. To effectively evaluate these mutations with an ion screen in the future, it is necessary to develop a screen that is based on synthetic media and controls that are also in design for homotrimeric α ENaC. Before mutations can be adequately analyzed, it is vital that controls are established. Therefore, this study specifically focused on creating a standard baseline of ion effects at various pH values and temperatures for functional homotrimeric α ENaC. It is hypothesized that addition of excess Na^+ , Cl^- , or H^+ ions will cause intermediate changes in growth in comparison to equal total concentrations of NaCl alone. In each case, it is specifically hypothesized that these intermediate changes will manifest as decreased sodium influx via ENaC, allowing for increased yeast cell growth in comparison to equal NaCl concentrations.

Vector Preparation/Transformation

Alpha ENaC was previously cloned into vector pYES2NT/A to be analyzed as a homotrimeric configuration and individually in future heterotrimeric configurations.

Properties of this vector (Figure 6) include a galactose promoter to initiate expression of the vector, an ampicillin resistance gene and URA3 marker to allow for selection of transformed bacteria and yeast cells, respectively, and a 2 μ origin of replication that denotes a high copy number of the plasmid, typically between 30-50 copies per cell. In frame with cloned α ENaC is the Xpress epitope that allows for identification of α ENaC in expression studies.

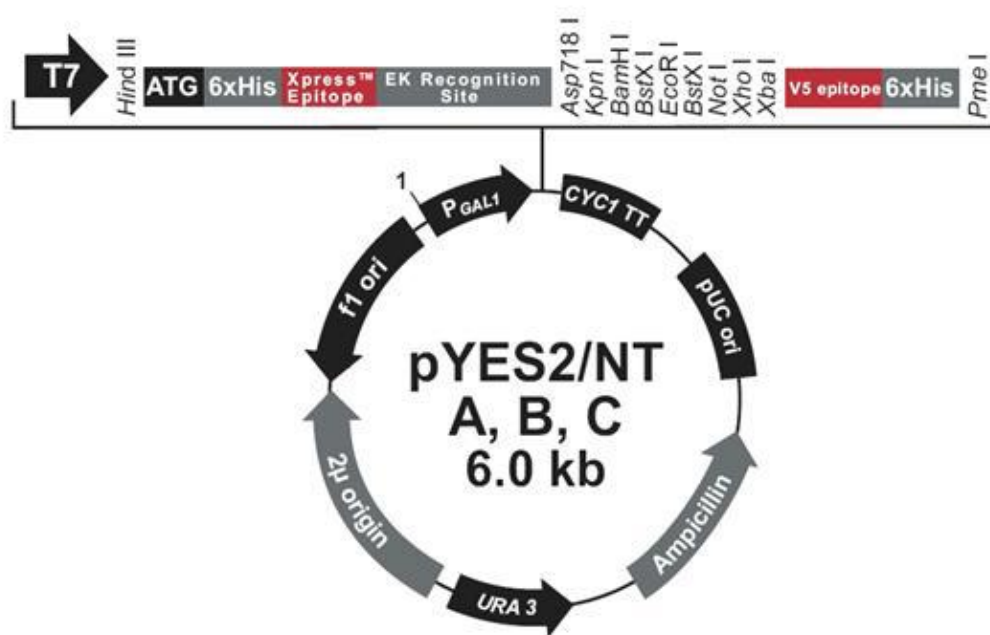


Figure 6. Vector Map of pYES2NT/A. α ENaC was subcloned at the designated restriction site.

E. coli cells were used to amplify concentrations of plasmid DNA. For both control pYES2/NT/A (Empty Vector) and pYES2/NT/ α ENaC, competent Top10 *E. coli* cells were heat shocked with 1-3 μ g of plasmids. For each plasmid transformation, growth in excess of 50+ colonies was observed. Selections of individual colonies were used in plasmid isolation to regenerate plasmid stocks for yeast studies.

A single colony from heat shock transformation into *E. coli* was selected and used to inoculate a 5 mL overnight in preparation for plasmid isolation with Qiagen QIAprep Spin Miniprep kit (Valencia, CA). At the culmination of the manufacturers protocol, elution with 50 μ L warm water resulted in recovery of 7.5 – 32 μ g of plasmid DNA from chromatographic columns.

Plasmid isolations were analyzed via horizontal gel electrophoresis. The migration of cloned vector pYES2NT/ α ENaC in a 1% (w/v) agarose gel corresponds to its respective size of 8000 bp (Figure 7).

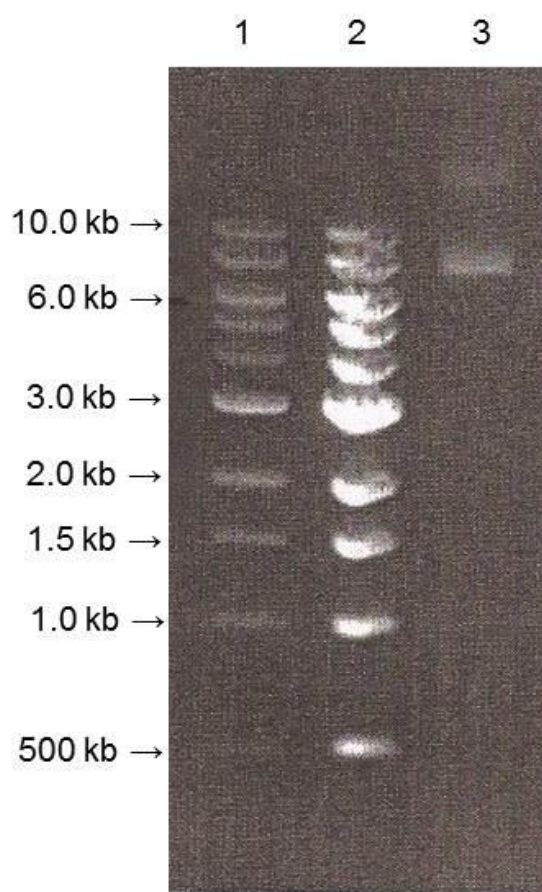


Figure 7. Gel electrophoresis of pYES2/NT/ α ENaC. Lane 1- 1kb DNA ladder, Lane 2- 1kb DNA ladder, Lane 3 - uncut pYES2/NT/ α ENaC plasmid DNA.

With the modified protocol from Soni, *et al.* (1993), a 5 mL YPDA overnight culture of yeast strain S1-InsE4A was grown in preparation for rapid transfection with 0.25 - 2.5 mg plasmid DNA. For each single plasmid transfection, 20+ colonies were seen after incubation at 30°C for 3 days (Figure 8). Single colonies could then be selected to form patch plates (Figure 9) for experimental use.

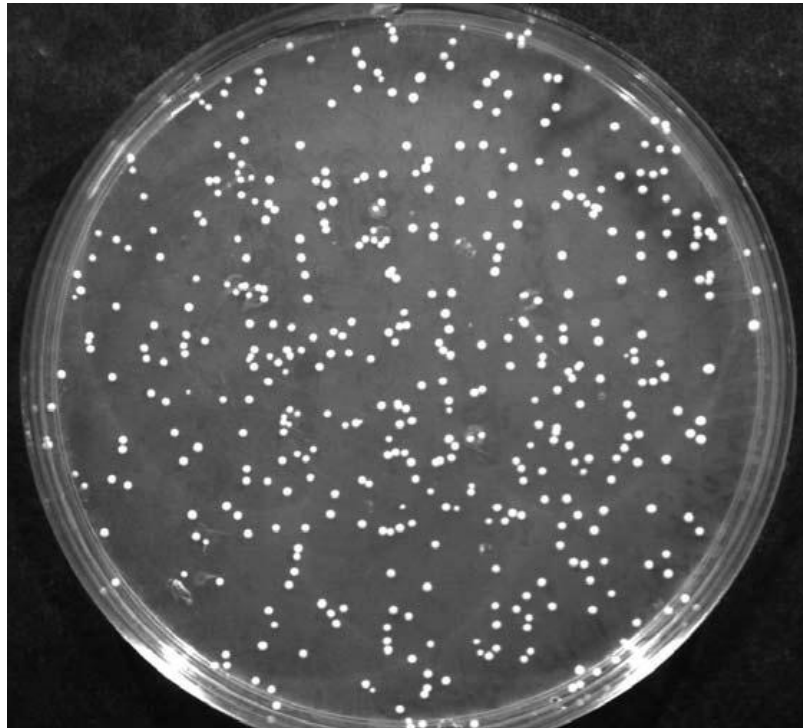


Figure 8. Successful rapid transfection into stationary phase *S. cerevisiae* yeast cells with pYES2NT/ α ENaC.

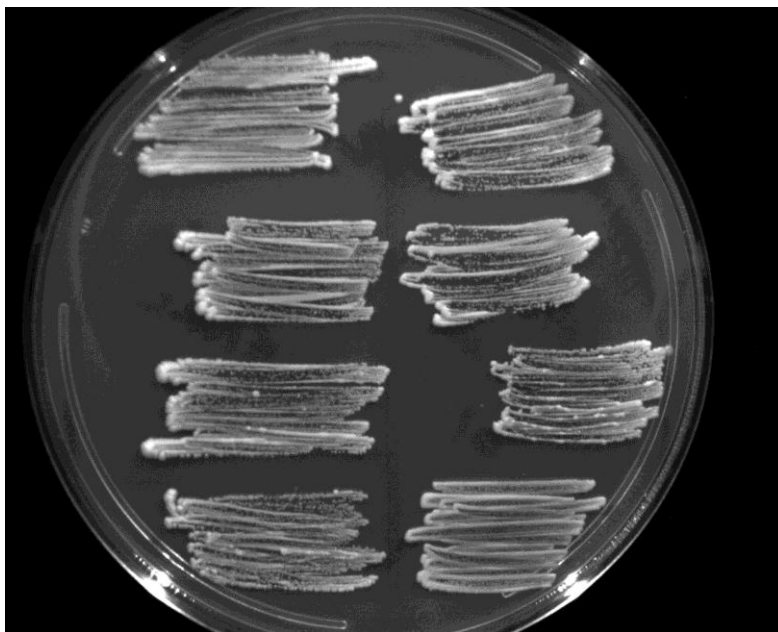


Figure 9. Patch plate of pYes2/NT/ α ENaC after transfection into *S. cerevisiae*.

Yeast Dilution Pronging Assay

For all dilution pronging assays, *S. cerevisiae* cells were transfected with pYES2/NT/A (empty vector) or pYES2/NT/ α ENaC and pronged onto control plates containing 2% glucose minus uracil or 2% galactose minus uracil with the following basal amounts of ions included in plate media: 2 mM Na⁺, 4 mM Cl⁻, 7 mM K⁺, and 80 mM NH₄⁺. Molarity concentrations listed at 0.25 M and 0.5 M were in addition to the basal amounts included in the media and do not represent the final molarity concentration within each plate. All plates were approximately pH 5.2 and were adjusted with KOH for pH studies only. For all edited figures, images are cropped from the same growth plate. Yeast contains several potassium channels and two sodium channels to maintain ionic and liquid homeostasis within the cell (30, 31, 32). These sodium channels are not

epithelia channels and although absorb sodium, are characteristically different, placing them in alternate superfamilies other than the ENaC/Degenerin channels (30).

Conditions of high solute concentrations in yeast induce a state of water stress, otherwise known as hyperosmotic shock. *S. cerevisiae* accommodate for this environmental stress by increasing the absorption of compatible solutes such as K^+ , Na^+ , glycerol and trehalose, all of which help maintain low cytosolic water activity (32). These solutes, particularly glycerol, help maintain the crystal state of membrane phospholipids and help stabilize membrane and intracellular proteins (32). The effects of ion absorptions in this study were controlled for with the empty vector. ENaC is the only variable channel between yeast containing control empty vector versus α ENaC. Therefore, any differences in yeast growth phenotypes were primarily contributed to permeability through ENaC channels.

Equal amounts of growth were observed between empty vector and α ENaC on 2% glucose (B), but a slight decrease in colony size was seen for cells expressing α ENaC in comparison to empty vector on 2% galactose (Figure 10A). An equal number of yeast cells were pronged between each column of α ENaC and control. The absence of growth in colonies for α ENaC indicates cell death while colony growth indicates cell survival. Colony diameter is an indication of survival growth rate and should be taken into consideration for the analysis of ion effects on yeast growth inhibition. However, colony size can only be compared between α ENaC and its corresponding vector control, not between pronging on various plates. pYES2/NT/A (empty vector) contained a galactose promoter, initiating expression of α ENaC on galactose selective plates, but not on glucose selective plates. Basal levels of Na^+ within media ingredients amount to 2 mM

and caused a very slight decrease in growth of cells expressing α ENaC over empty vector for galactose plates (33). Most yeast transformants in this experiment grew at similar viability for 2% glucose selective media since there was no expression of α ENaC. Therefore, the 2% glucose images for the remainder of the pronging analysis will be provided to show growth controls, but will not be further discussed unless a variation in growth was present.

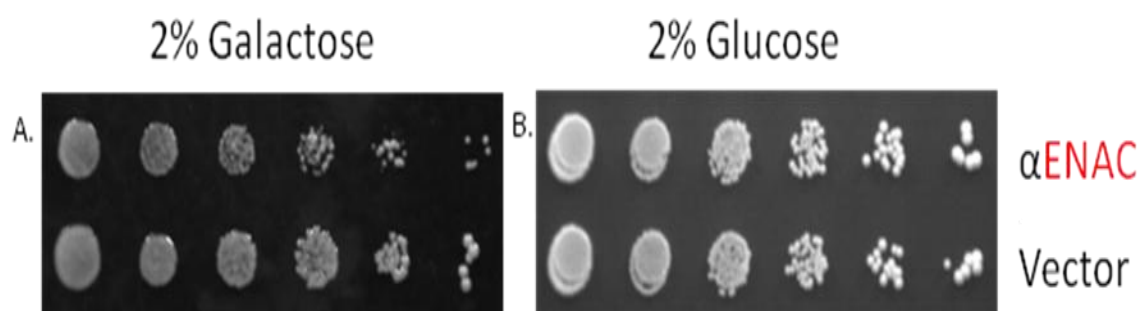


Figure 10. Control prongings without additional NaCl to basal amount. Pronging of α ENaC (top) and empty vector (bottom) in 2% galactose (A) and 2% glucose (B) media. Grown at 30 °C between 2-4 days.

Dilution Pronging Assay: Standard 0.25 M and 0.5 M NaCl Controls

Pronging assays were performed using various concentrations of NaCl: a basal molarity 2 mM with no addition of NaCl, 0.25 M and 0.5 M to evaluate sodium self-inhibition (Figure 11). In the presence of 0.25 M (B) and 0.5 M NaCl (C), α ENaC showed increasing growth inhibition with smaller colony diameters in comparison to empty vector. This did not correlate with hypothesis of sodium self-inhibition and it is possible that at these concentrations of NaCl the negative feedback mechanism is saturated and therefore perpetually active.

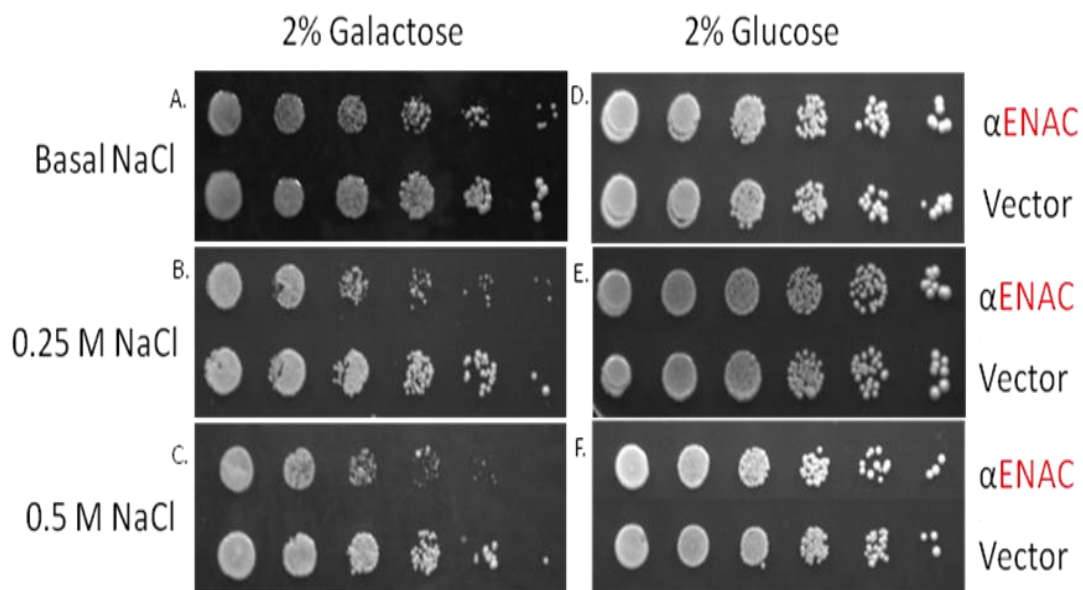


Figure 11. Standard NaCl control prongings. α ENaC (top) and empty vector (bottom) in 2% galactose or glucose media with basal NaCl, 0.25 M NaCl, and 0.5 M NaCl. Growth at 30 °C between 4-5 days.

Dilution Pronging Assay: Effects of Li^+ as a competitive inhibitor of sodium

Various concentrations of Li^+ were added to the media at 0.25 M and 0.5 M, and in combination with NaCl, at 0.25 M each, to analyze the competitive effects of Li^+ with Na^+ in yeast (Figure 12). In the presence of 0.25 M LiCl (Figure 12D), yeast with both α ENaC and empty vector on 2% galactose showed increased growth inhibition in comparison to the 2% glucose control. Glucose is the preferred carbon source of yeast. However, even in the presence of glucose, Li^+ ions had a detrimental effect on yeast growth as seen in Figure 12I and 12J. Due to the size of Li^+ , it was apparent that it was passing through other native ion channels in yeast (30, 33). In combination with secondary carbon source, galactose, toxic Li^+ ions proved more detrimental to yeast

growth. Increasing effects were seen in α ENaC yeast as higher concentrations of Li^+ were able to enter the cell through ENaC.

In comparison to 0.25 M LiCl (D) both 0.25 M (C) and 0.5 M (B) NaCl showed more viable growth for empty vector and α ENaC. The addition of 0.25 M LiCl with 0.25 M NaCl (E) minimized growth inhibition for both α ENaC and empty vector in comparison to 0.25 M LiCl (D), but increased growth inhibition in comparison to 0.25 M NaCl (C) and 0.5 M NaCl (B). Li^+ ions are smaller than Na^+ ions and therefore can pass readily through α ENaC channels causing harmful effects to the yeast cell. This would correspond with increased growth inhibition in α ENaC (D), but what was unexpected were the increased growth inhibition effects of 0.25 M LiCl on the empty vector (D). Li^+ ions were not entering the cell via ENaC since they are not present in the cell membrane of the empty vector. Therefore, as seen on glucose pronging, Li^+ ions must have entered through alternative native channels within the yeast cell. The decrease in growth inhibition for the empty vector in the combination of 0.25 M LiCl and 0.25 M NaCl (E) could be due to the blockage of these alternate channels by the presence of larger Na^+ ions. The decrease in yeast growth inhibition for α ENaC was likely due to the competition of Na^+ with Li^+ minimizing the intracellular concentration of Li^+ overall. Although excess intracellular Na^+ concentrations cause yeast growth inhibition, the effects are not as disruptive to physiological conditions as increased intracellular Li^+ concentrations.

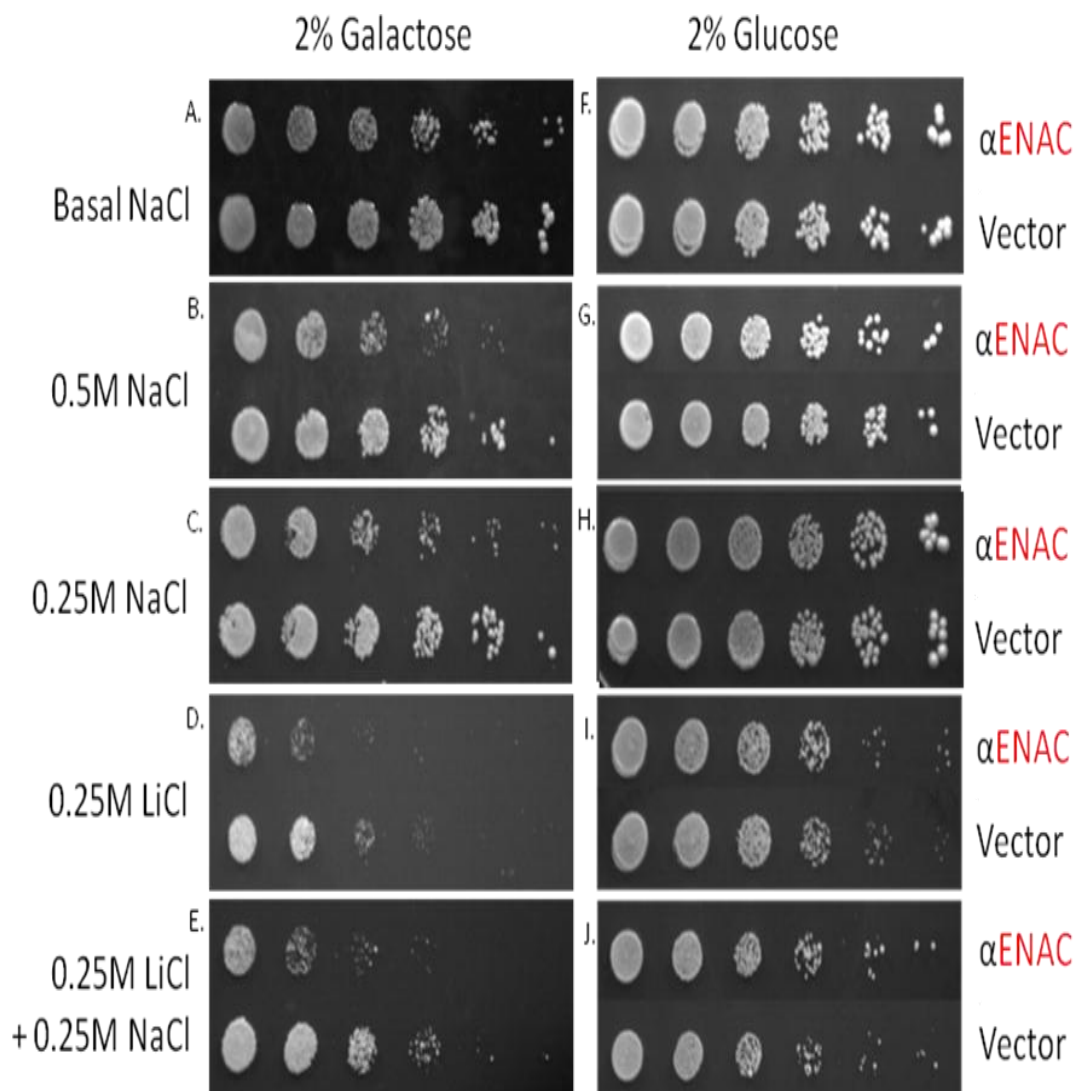


Figure 12. Competitive sodium inhibition with Li^+ . Pronging of α ENaC above empty vector negative control in 2% glucose or galactose media with basal NaCl (A), 0.25 M NaCl (C), 0.5 M NaCl (B), 0.25 M LiCl (D), and 0.5 M total combined concentration of 0.25 M LiCl and 0.25 M NaCl (E). Growth at 30°C between 4-7 days.

Dilution Pronging Assay: Effects of NH_4^+ and K^+ on ENaC regulation.

αENaC was analyzed in the presences of excess K^+ and NH_4^+ ions, respectively, to investigate whether possible interactions with ENaC that might result in up or down regulation. Individually, excess NH_4^+ ions at 0.25 M (Figure 13C) showed more robust growth like control with basal NaCl (A), indicating no individual effects of NH_4^+ ions on ENaC in the absence of additional Na^+ ions. When combined with equal amounts of 0.25 M NaCl (D), yeast growth inhibition for αENaC decreased in comparison to 0.25 M NaCl (B), indicating possible promotion of sodium self-inhibition. This is contrary to hypothesis that excess NH_4^+ ions would contribute to increased sodium influx. To further investigate this, equal concentrations of 0.5 M NH_4^+ were pronged with 0.5 M NaCl (E), but showed increased yeast growth inhibition similar to 0.5 M NaCl (F) without additional NH_4^+ ions. The change in yeast growth phenotype with increasing salt concentration could be due to saturation at molarities over 0.25 M combinations and should be investigated further. Overall, NH_4^+ ions in excess were not contributing to either up or down regulation of ENaC. NH_4^+ is present at higher concentrations within the lumen during physiological states of acidosis and was suspected to model excess protons as they minimize sodium self-inhibition. It is possible that contradictions to this hypothesis are due to the variation in species response to pH regulation (25).

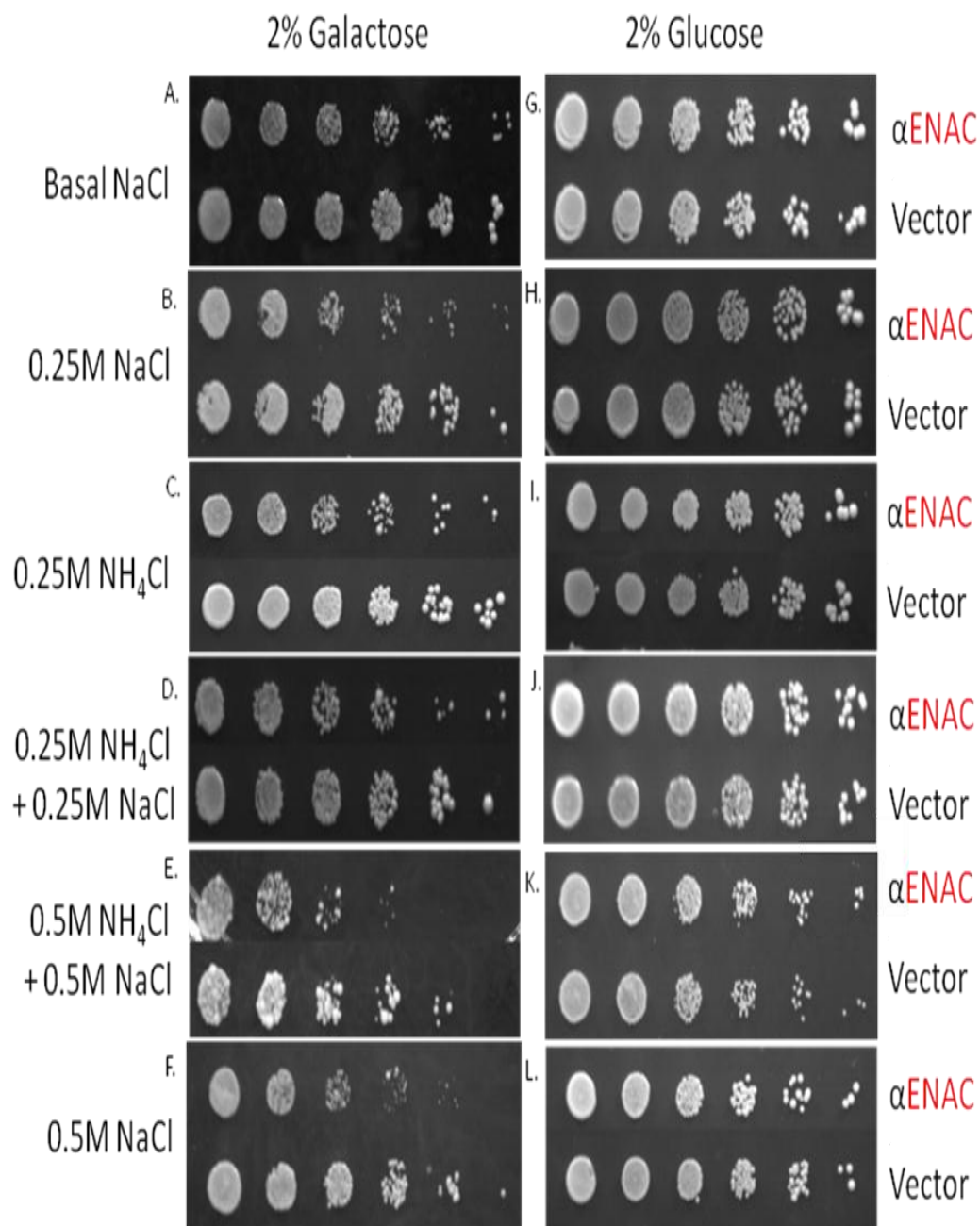


Figure 13. Prongings of NH_4^+ ions effect on ENaC. Pronging of αENaC above empty vector negative control in 2% galactose or glucose media with basal salt (A) and with various salt concentrations: 0.25 M NaCl (B), 0.25 M NH_4Cl (C), 0.25 M NH_4Cl + 0.25 M NaCl (D), 0.5 M NH_4Cl + 0.5 M NaCl (E), and 0.5 M NaCl (F). Growth at 30 °C for 2-5 days.

In an effort to elucidate a possible regulatory mechanism triggered by K^+ ions were added to the media at varying concentrations of 0.25 M, 0.5 M, and mixed with equal 0.25 M concentrations of NaCl (Figure 14). Images of 0.5 M combinations are not shown because the 1.0 M total concentration of 0.5 M KCl or NH_4Cl with 0.5 M NaCl proved unfavorable for yeast empty vector growth on galactose plates. This is likely due to the high salt concentration not being conducive with physiological conditions in combination with galactose as a secondary carbon source. In Figure 14, 0.25 M additional KCl (C) to the basal 7 mM K^+ ions included in the media showed increased growth inhibition for $\alpha ENaC$. There was no additional NaCl added to the media and phenotypes were expected to model basal NaCl control (A). This contrast is likely due to K^+ passage through ENaC. K^+ ions are larger than Na^+ ions and have a greater sphere of solvation once hydrated. ENaC is thought to be highly selective for Na^+ due to the exact alignment of solvated Na^+ with amino acids of the extracellular loop of ENaC. It could be that without competition of Na^+ , excess K^+ ions are able to collect around the extracellular loop in such an orientation that the energy of desolvation is decreased and K^+ passage through ENaC can occur. KCl combinations with 0.25 M equal concentration of NaCl (D) grew at very similar patterns to 0.25 M NaCl (B). This shows that in competition with Na^+ , K^+ ions have less of an opportunity to orient themselves for passage through ENaC. This growth phenotype is also in contrast to hypothesis that K^+ could be involved in upregulation of ENaC, which would phenotype as increased growth inhibition. It is possible that efforts to repair overall high intracellular ion concentrations through passive efflux of K^+ out of the cell would be counteracted by an upregulation of Na^+ influx.

To suspect roles in regulation of ENaC from either ion, yeast growth at 0.25 M combinations in Figure 13 and 14 would be more robust than 0.25 M NaCl alone.

However, all model one another, suggesting that K^+ and NH_4^+ do not likely play a role in either up or down regulation of α ENaC at 30°C.

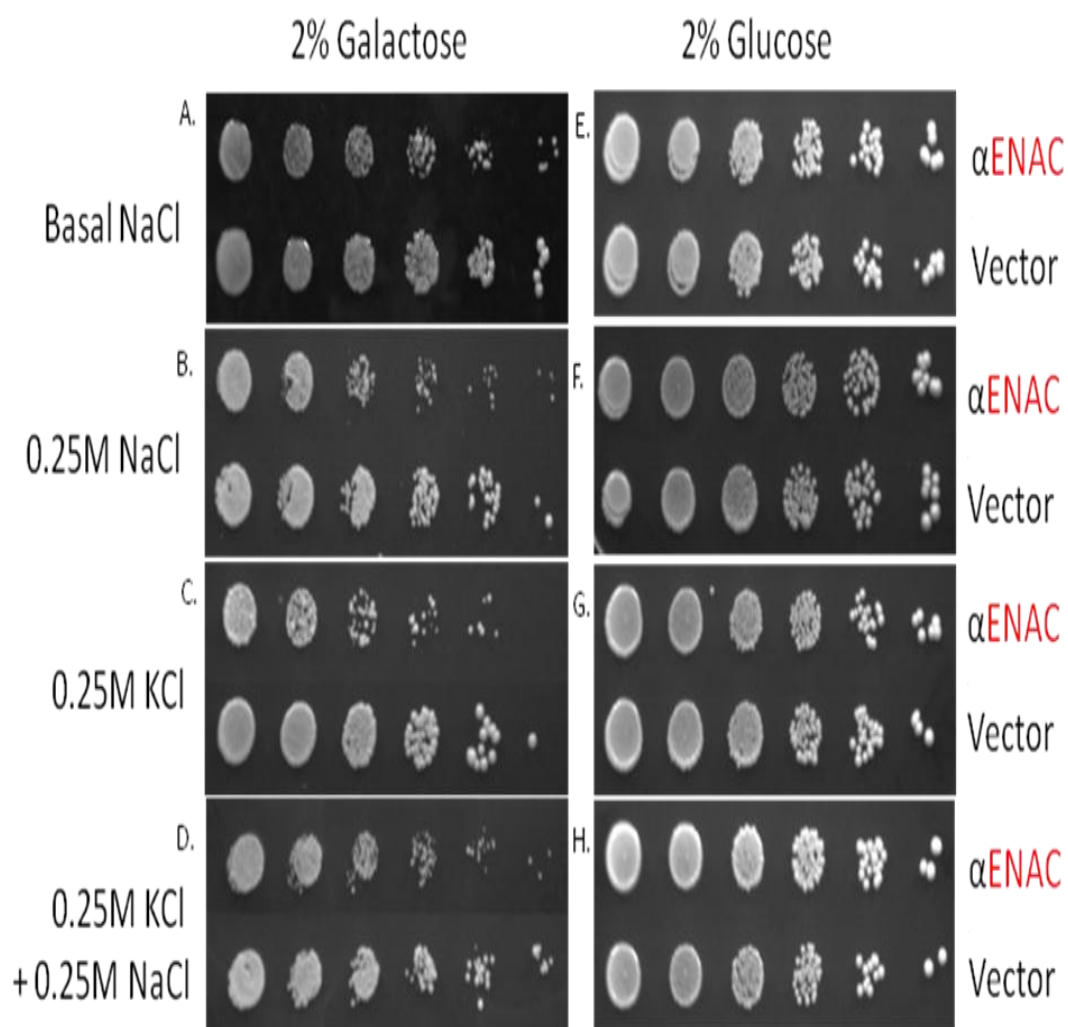


Figure 14. Prongings of K^+ ions effect on ENaC. Pronging of α ENaC above empty vector negative control in 2% galactose or glucose media with basal salt (A) and with various salt concentrations: 0.25 M NaCl (B), 0.25 M KCl (C), 0.25 M KCl + 0.25 M NaCl (D). Growth at 30°C for 2-5 days.

Dilution Pronging Assay: Effects of direct sodium inhibition and indirect sodium self-inhibition through additive effects of Cl^- .

The direct effects of Cl^- ions on ENaC were analyzed to investigate possible structural similarities to ASIC, which contains intersubunit Cl^- binding pockets that modulate channel activity (25). With a total Cl^- concentration of 0.25 M (Figure 15B and C), there was a slight increase in yeast growth inhibition in comparison to empty vectors and αENaC at basal NaCl (A), which contained 2 mM Na^+ and 4 mM Cl^- , but the extent of the growth inhibition was not the same. This indicated that Cl^- ions were not responsible for this effect considering that concentrations of Cl^- ions remained constant between Figure 15B and C. However, when Cl^- ion concentration was doubled to 0.5 M from the combination of 0.25 M NH_4Cl and 0.25 M NaCl (E), growth inhibition decreased in comparison to 0.25 M NaCl (B). If Cl^- alone were to affect ENaC function, then a decrease in growth inhibition would be expected when Cl^- concentrations were doubled. To confirm this correlation with hypothesis, Cl^- ion concentrations were again doubled to 0.5 M from the combination of 0.25 M KCl and 0.25 M NaCl (D). However, this second combination showed growth inhibition similar in comparison to 0.25 M NaCl (B) without a decrease. Due to inconsistency between salt combinations, a direct method of regulation from Cl^- ions could not be confirmed. It could be that this mechanism does in fact exist, but at 0.25 M the binding pockets for Cl^- were saturated, preventing any further phenotype changes at 0.5 M.

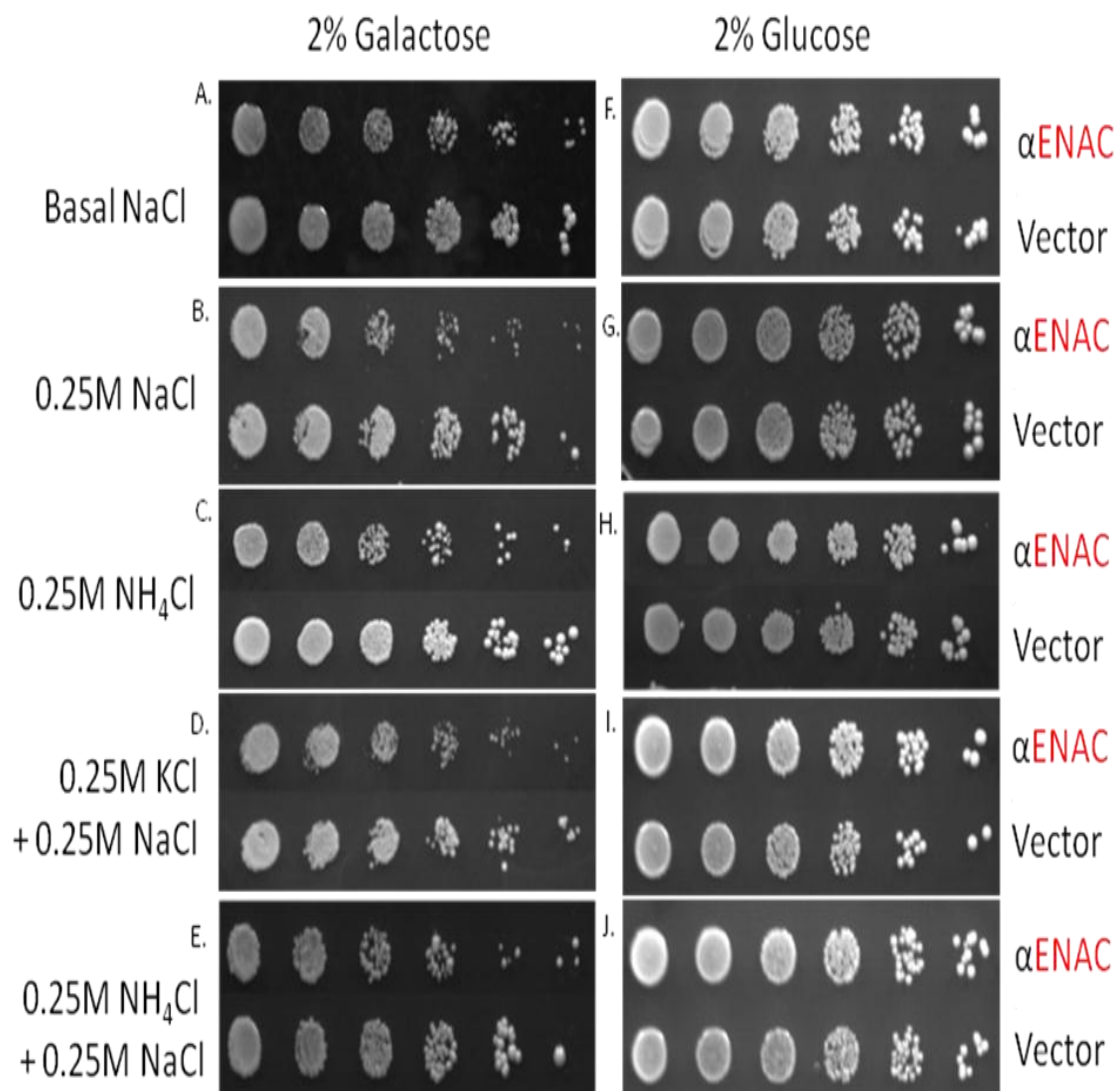


Figure 15. Prongings of direct sodium inhibition by Cl^- ions. αENaC above empty vector negative control in 2% galactose or glucose media basal salt (A) and with various salt concentrations: 0.25 M NaCl (B), 0.25 M NH_4Cl (C), 0.25 M KCl and 0.25 M NaCl (D), 0.25 M NH_4Cl + 0.25 M NaCl (E). Growth at 30 °C for 2-5 days.

To investigate indirect methods of regulation via promotion of sodium self-inhibition, Cl^- ions were examined in combination with different concentrations of Na^+ ions (Figure 16). At 0.25 M concentration of Na^+ and 0.5 M total concentration of Cl^-

(C), there was an increase in growth inhibition in comparison to basal NaCl (A), containing 2 mM Na⁺ and 4 mM Cl⁻. The concentration of Cl⁻ ions remained the same at 0.5 M and Na⁺ was increased to 0.5 M (C) and an even further increase in growth inhibition was observed. It was hypothesized that Cl⁻ would promote sodium self-inhibition, so as Na⁺ concentrations increased in the presence of constant Cl⁻, a decrease in growth inhibition was expected. This was not seen as Figure 16B and D showed increased growth inhibition. Variation from the hypothesis could also be similar to explanations for lack of direct effects of Cl⁻, that interactions with the extracellular loop might be saturated at 0.25 M which would prevent any significant change at 0.5 M.

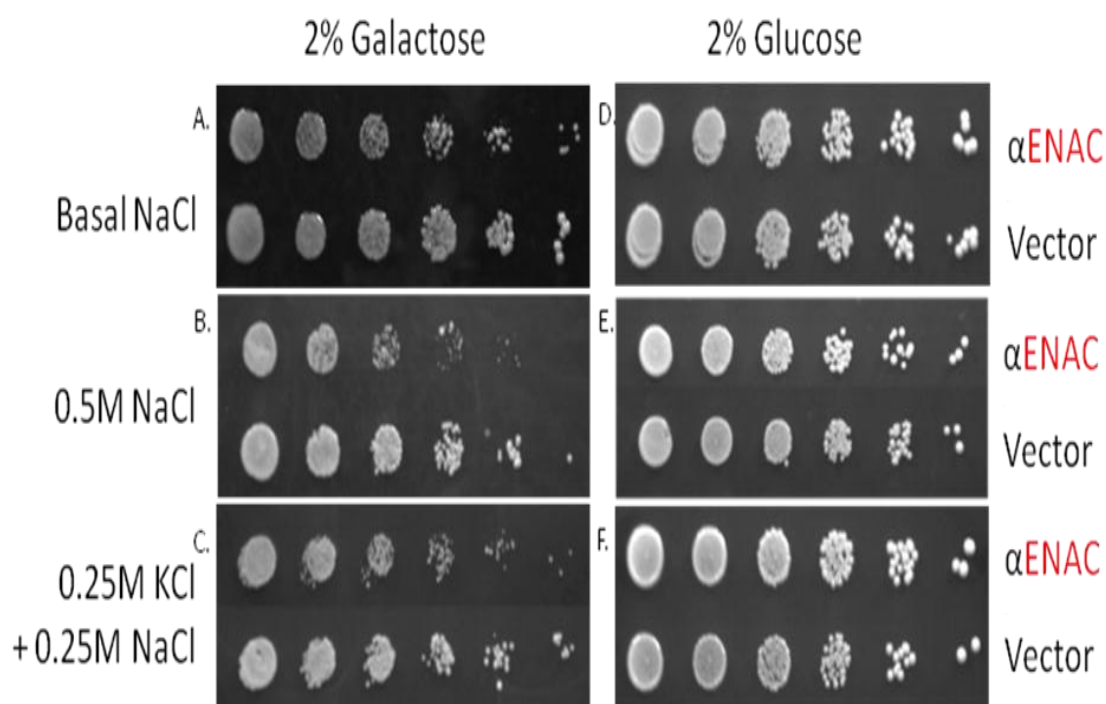


Figure 16. Pronging analysis of sodium self-inhibition from Cl⁻ ions with excess Na⁺ ions. α ENaC above empty vector negative control in 2% galactose or glucose media with basal salt (A) and with various salt concentrations: 0.5 M NaCl (B), 0.25 M KCl + 0.25 M NaCl (C). Growth at 30°C for 2-5 days.

Dilution Pronging Assay: Effects of pH levels 5, 6, 7, and 8 with 0.25 M and 0.5 M NaCl.

Regulation of ENaC with excess protons was evaluated at pH 5, 6, 7, and 8 at both 0.25 M (Figure 17) and 0.5 M (Figure 18) additional NaCl. Consistent growth on 2% glucose was seen for all pH variations. However, pH 8 showed no growth of any kind with 2% galactose as a carbon source at 0.5 M (Figure 18D). Media plates utilized for yeast growth contain a pH approximately at 5.2 and were used as controls to evaluate pH levels 6 and 7. Yeast growth at pH 6 on 2% galactose resembled growth at control pH 5 on 2% galactose with a slight decrease in growth inhibition for both molarities (Figure 17B & 18B). Yeast growth at pH level 7 on 2% galactose resembled growth at control pH 5 on 2% galactose at 0.25 M without an increase or decrease in growth inhibition (Figure 17C), but at pH 7 at 0.5 M showed an increase in yeast growth inhibition (Figure 18C). Research has shown variation in species response to pH modulation of sodium self-inhibition accounting for plausible differences from the hypothesis that self-inhibition will consistently increase as pH becomes more alkaline (26). Initial literature studies showed that human epithelial cells responded to pH modulation of sodium self-inhibition, but that rat $\alpha\beta\gamma$ ENaC showed no sensitivity. This was speculated to be due to variations in ENaC between the two species (26). This study used mouse $\alpha\beta\gamma$ ENaC, but as a homotrimeric α ENaC protein, which led to the investigation of pH as a candidate for ENaC regulation for this study. It seems that in mouse homotrimeric α ENaC, there was a decrease in growth inhibition as pH levels became more alkaline from pH 5 to pH 6, which corresponds with literature for human heterotrimeric $\alpha\beta\gamma$ ENaC. However, there was a contrast to hypothesis at pH 7 as yeast

growth inhibition increased from pH 6 for α ENaC. This could be due to an overall deprotonation of functional groups within amino acids that are critical to the structure of ENaC, creating a more porous structure that would increase Na^+ influx into the cell. At 0.5 M, there was a slight decrease in yeast empty vector survival at pH 7 (Figure 18C) and complete lack of yeast survival at pH 8 (D) for both empty vector and α ENaC. This indicates that other variables in physiological conditions are responsible for yeast growth inhibition, such as galactose transport into the cell. For some yeast strains, galactose transporters are symporters with H^+ ions (33). It is likely that as alkaline conditions increase, there are fewer H^+ ions free in the media to facilitate in galactose transport into the cell.

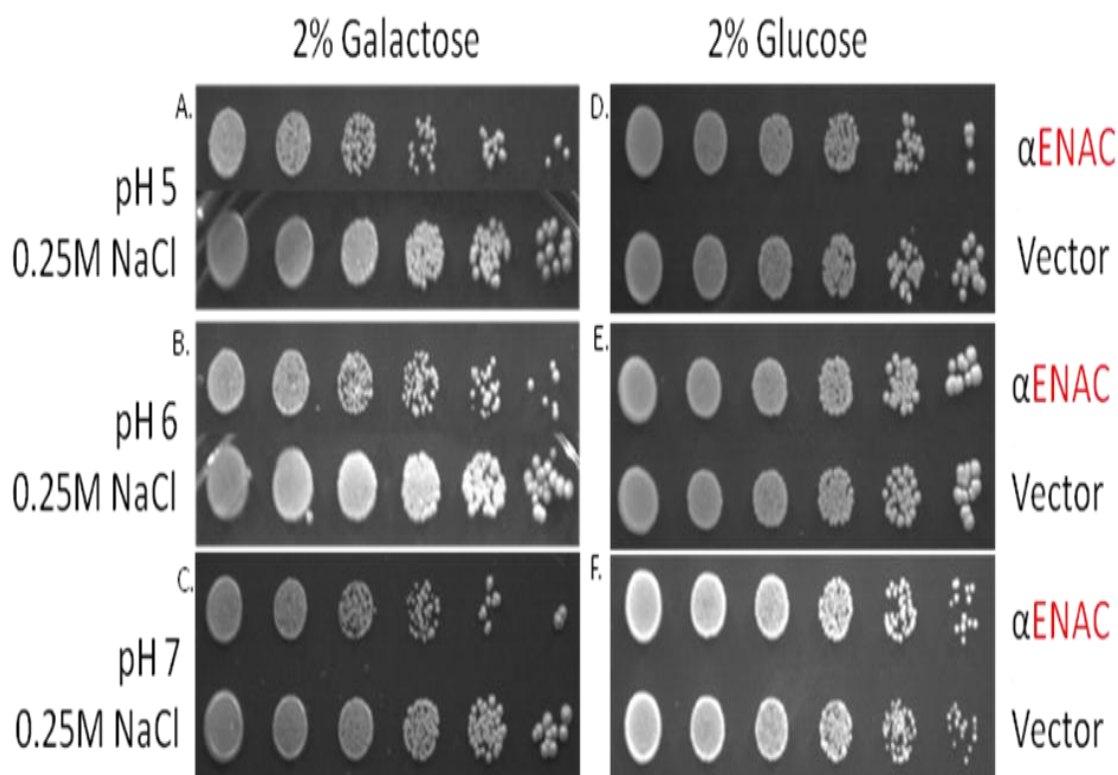


Figure 17. Pronging analysis at various pH levels with additional 0.25 M NaCl. α ENaC above empty vector negative control in 2% galactose or glucose media with 0.25 M NaCl at approximately pH 5 (A), pH 6 (B), and pH 7 (C). Growth at 30 °C for 2-5 days.

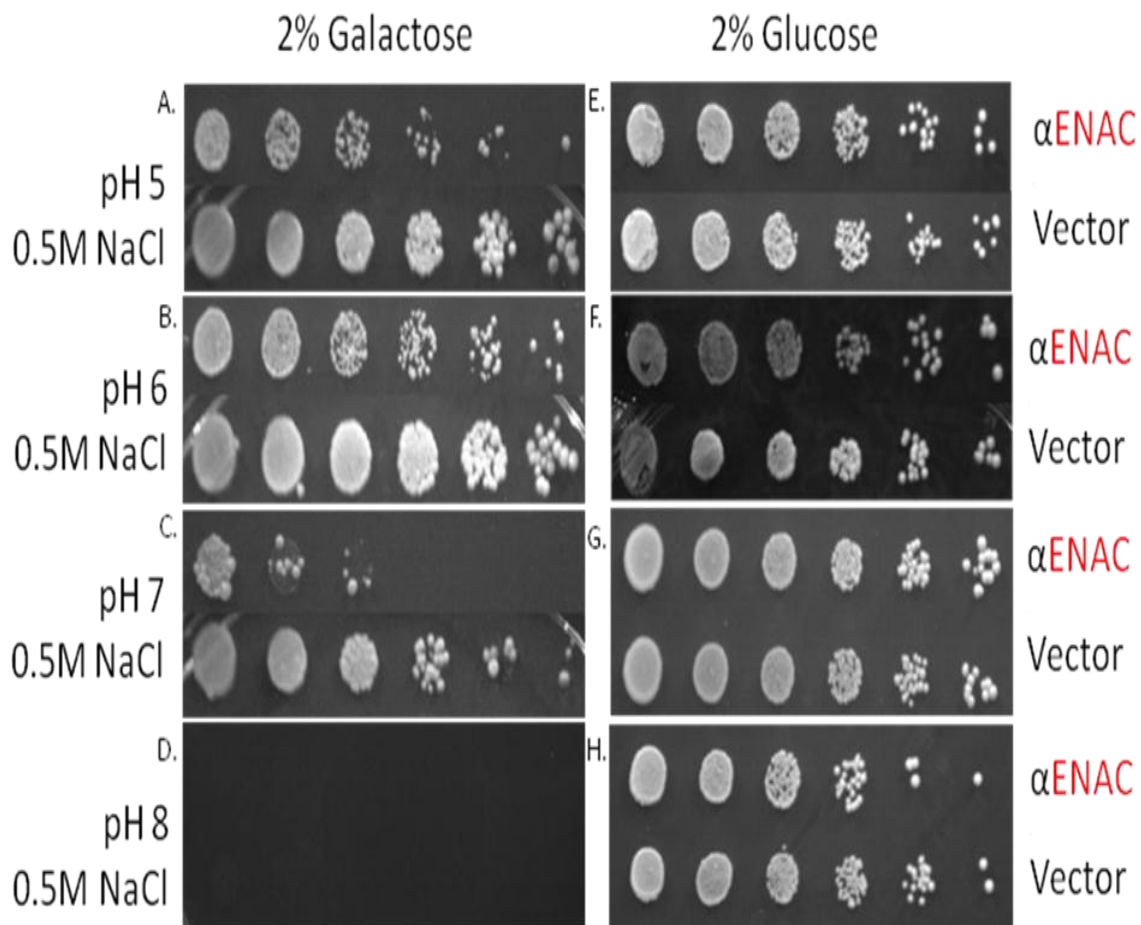


Figure 18. Pronging analysis at various pH levels with additional 0.5 M NaCl. α ENaC above empty vector negative control in 2% galactose or glucose media with 0.5 M NaCl at approximately pH 5 (A), pH 6 (B), pH 7 (C), and pH 8 (D). Growth at 30 °C for 2-5 days.

Dilution Pronging Assay: Ion regulation at 16 °C and 37 °C.

In yeast model systems, optimal growth occurs at 30 °C. Ranges in growth temperatures provide amplified phenotypes, allowing for a clear and timely identification of dysfunctional ENaC (34). In an effort to clarify the role of ions in regulation of ENaC, pronging assays were performed at 16 °C and 37 °C on 2% galactose (Figure 19). All

ion combinations of 0.25 M and 0.5 M on 2% glucose plates grew at 16 °C and 37 °C with up to 12 days necessary for growth at 16 °C and 2 days at 37 °C (Figure 20). For every 2% glucose pronging at 16 °C and 37 °C, phenotypes modeled growth seen at 30 °C. On galactose however, extreme decrease of growth and survival were seen at 37 °C (Figure 19G-I). Empty vector showed robust growth, but α ENaC showed amplified growth inhibition in comparison to 30 °C (D-F) concentrations with only basal NaCl (G), allowing for minimal changes to be detected with increased NaCl concentrations to 0.25 M (B) and 0.5 M (I). It is possible that excess heat dehydrated the media and induced hyperosmotic shock to the cells, leading to increased sodium influx from the basal ingredients of yeast media to help maintain low cytosolic water activity (32). This would result in a more amplified phenotype without the addition of NaCl. It is also possible that weak interactions between amino acids maintaining the structure were disrupted at the higher temperature, producing a more porous protein. Once increased NaCl was added, for both 0.25 M and 0.5 M plate at 37°C, rare temperature resistant colonies were observed. This was consistent over multiple trials, removing speculation of contamination. These papilla colonies were a result of random mutations that allowed for more viable growth of the organism under these conditions. The frequency of mutations in yeast cells is $\sim 1:10^6$ cells, and considering that there were close to a million cells pronged in the first two columns of each plate, it is not unlikely that these randomly occurring mutations increased resistance to NaCl or high temperatures.

Galactose plates at 16 °C with NaCl additions at 0.25 M (Figure 19B) and 0.5 M (C) grew in a similar growth pattern as 30 °C (E-F) but with up to 14 days necessary for growth. Oddly, without salt, there is minimal growth seen for the empty vector and only

the first two to three columns of cell quantities displaying visible growth for α ENaC (A). Yeast growth overall increases (A-C) as salt is added to the media indicating that additional NaCl must increase the viability of yeast at lower temperatures. Combination plates with a total of 1.0 M salts showed close to no growth after 14 days and LiCl treated cells did not grow at either 0.25 M or 0.5 M combinations up to 14 days (data not shown). Ultimately, temperature variations provided amplified phenotypes seen at 30° C and could be used in future studies. However, variables contributing to growth inhibition in control empty vector with basal NaCl need to be further investigated before use.

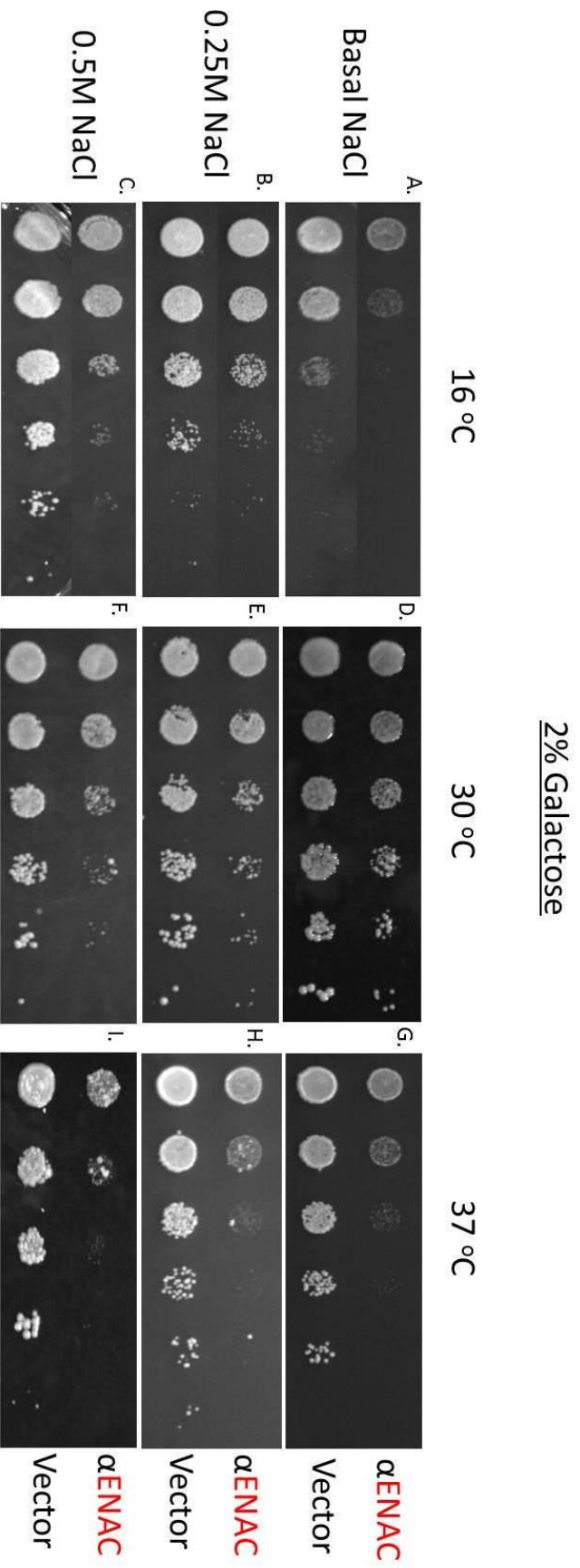


Figure 19. Ion regulation at 16 °C and 37 °C on 2% galactose. αENAC above empty vector negative control in 2% galactose media with basal salt (A, D, G), with 0.25 M additional NaCl (B, E, H), and 0.5 M additional NaCl (C, F, I). Growth at 16 °C (A, B, C), 30 °C (D, E, F), and 37 °C (G, H, I) for 2-10 days.

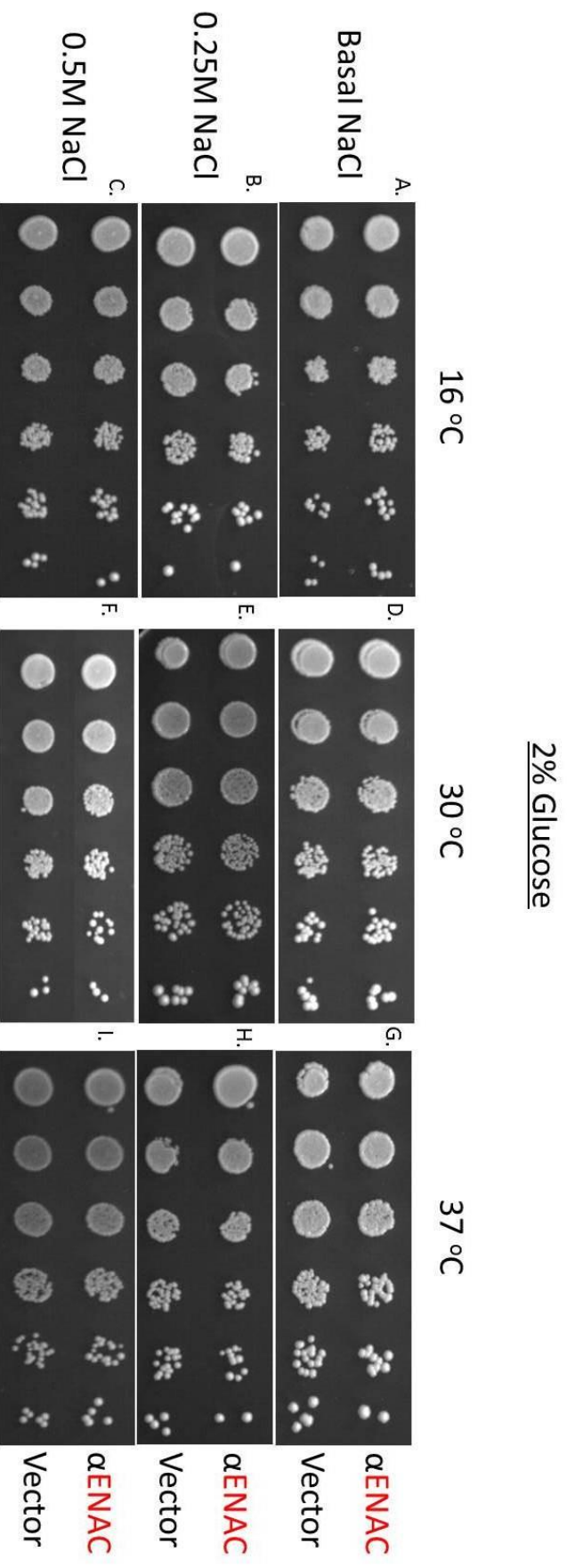


Figure 20. Ion regulation at 16 °C and 37 °C on glucose. αENAC above empty vector negative control in 2% glucose media with basal salt (A, D, G), with 0.25 M additional NaCl (B, E, H), and 0.5 M additional NaCl (C, F, I). Growth at 16 °C (A, B, C), 30 °C (D, E, F), and 37 °C (G, H, I) for 2-10 days.

Overall, differences in results observed in this study from proposed hypotheses could be due to the study of ENaC as a homotrimeric α ENaC as opposed to heterotrimeric $\alpha\beta\gamma$ ENaC as studied in the literature. They could also possibly be due to the structure of yeast model organisms in comparison to more advanced eukaryotic systems where ENaC is more commonly found. Mutations to the alpha subunit of ENaC have been shown to affect sodium self-inhibition in patch clamp studies with $\alpha\beta\gamma$ ENaC (24, 35). With the stoichiometry unknown, it can only be speculated that perhaps there are critical interactions between the three subunits that, when absent, change allosteric binding with extracellular ions. Perhaps with $\alpha\beta\gamma$ ENaC as the most permeable configuration to sodium influx, and therefore the most susceptible to rapid changes in physiological states, sodium self-inhibition is a regulation method that has evolved more prominently for the heterotrimeric configuration of the protein. It is also possible that with yeast as a model system, certain machinery involved in regulatory maintenance of intracellular concentrations are not present, preventing clear study and observation of self-inhibition in ENaC. Among these could be the absence of a sodium/potassium pump in yeast that is seen in the basolateral membrane of epithelial cells in mammalian systems (33). High intracellular salt concentrations cause growth inhibition. Sodium influx could be dampened by a self-inhibition mechanism, but without a sodium/potassium pump, the yeast cannot return to a normal physiological state to show recovery of growth as less sodium enters the cell. Another explanation is that in the presence of standard high sodium concentrations as seen at 0.25 M, that an hypothesized allosteric site providing negative feedback of sodium influx would be perpetually active. This could be possible

considering the sodium concentrations inside the distal tubule epithelial cells exist around 10 mM with concentration outside the cell in the kidney collecting duct ranging from 1-100 mM depending on volume depletion or excess (25, 36). In essence, the positive control utilized in this ion screen and in previous mutation pronging assays could represent a slightly decreased rate of sodium influx due to finite tuning of sodium self-inhibition that is consistently taking place.

CHAPTER IV

CONCLUSION

The epithelial sodium channel is a critical component to fluid homeostasis, however low expression levels make it difficult to study in mammalian systems. Yeast cells are used as a recombinant system and provide a very useful visual screen for functional and dysfunctional ENaC. This screen has been successfully utilized in mutation studies to identify possible critical amino acids to the structure and function of ENaC. In an effort to clarify the role of monovalent and divalent cations in possible allosteric regulation through a negative feedback mechanism of sodium self-inhibition, a yeast screen using different ion combinations in media was developed for homotrimeric α ENaC. Patch clamping studies have shown the removal of sodium self-inhibition with mutations to amino acids, some of which are included in the alpha subunit alone (24, 35). Based on these studies, it was hypothesized that excess Na^+ , the presence of Cl^- , and NH_4^+ ions would promote sodium self-inhibition and decrease sodium influx into the cell. Alternatively, the presence of K^+ and a decrease in H^+ would minimize sodium self-inhibition and increase sodium influx. Li^+ as a sodium competitor was also analyzed. The addition of all ions in the study did not confer as hypothesized with the exception of Li^+ , which did show competitive inhibition with sodium through ENaC. It is possible that as a homotrimeric α ENaC, that alternative forms of ion regulation exist or that they

do not exist at all, reserved only for more porous $\alpha\beta\gamma$ ENaC configurations. Variations could also be seen due to lack of regulatory machinery within yeast that would assist in maintaining intracellular homeostasis in correlation with sodium self-inhibition. Another possibility would be that the lowest concentration of sodium in these yeast studies was too high and saturated sodium self-inhibition, preventing observation of changes in yeast phenotype with increased ion concentrations. High salt concentrations have proven useful for the amplified phenotypes of critical mutations, but perhaps in regulation studies, lower concentrations need to be analyzed with a much lower pronging dilution of yeast. In the future analysis of critical mutations to regulation mechanisms of extracellular ENaC, a screen with heterotrimeric $\alpha\beta\gamma$ ENaC should be developed to confirm that yeast as a model organism can provide consistent results with the literature. Currently, a baseline of ion effects on functional homotrimeric α ENaC has been established and mutations can be tested using the same α ENaC screen for observation at 30 °C to investigate if effects of these mutation with NaCl alone increase or decrease in the presence of K^+ , NH_4^+ , Li^+ , Cl^- or H^+ . Although the standard baseline of this screen varies from heterotrimeric studies in the literature, this screen is unique to homotrimeric α ENaC in yeast and can still provide insight to how critical amino acids identified from yeast screens are interacting within the extracellular loop and with other ions in their environment. Ultimately, this ion screen can be helpful in elucidating the structure and function of ENaC by further clarifying the critical nature of specific amino acids important to the overall stoichiometry of the protein.

REFERENCES

1. Rossier, B.C., Pradervand, S., Schild, L., and Hummler, E. (2002) *Annu. Rev. Physiol.* **64**, 877-897
2. Tong, Q., Booth, R.E., Worrell, R.T., and Stockand, J.D. (2004) *Renal Physiol.* **286**, 1232-1238
3. 22. CDC/National Health Center for Health Statistics. Center for Disease Control and Preventions. 2011 Oct. 19th. Available from: <http://www.cdc.gov/nchs/fastats/lcod.htm>
4. Post R., Sen A., Rosenthal A. (1965) *J Biol Chem* **240**, 1437-45
5. Kellenberger, S., and Schild, L. (2002) *Physiol. Rev.* **82**, 735-767
6. Bassilana, F., Champigny, G., Waldmann, R., de Weille, J.R., Heurteaux, C., and Lazdunski, M. (1997) *J. Biol. Chem.***272**, 28819-28822
7. Booth, R.E., Tong, Q., Medina, J., Snyder, P.M., Patel, P., and Stockand, J.D. (2003) *J. Biol. Chem.* **278**, 41376-41379
8. Kellenberger, S., Gautschi, I., and Schild, L. (2003) *Mol Pharmacol* **64**, 848-856
9. Stockand JD, Staruschenko A, Pochynyuk O, Booth RE, Silverthorn DU. *IUBMB Life* **2008**, 60, 620-8
10. Shehata, M.F. (2009) *Int. Arch. Med.* **2**, 28-37
11. Itzhak, M., Driscoll, M. D. (1999) *BioEssays* **21**, 568-578
12. Canessa, C.M., Schild, L.M., Buell, G., Thorens, B., Gautschi, I., Horisberger, J.D., and Rossier, B.C. (1994) *Nature (Lond.)* **367**, 463-467
13. McNicholas, C. and Canessa, C.M. (1997) *J. Gen. Physiol.* **109**, 681-692
14. Snyder, P. M. *Endocrine Reviews* **2002**, 23, 258-275
15. Asher, C., Wald, H., Rossier, B.C., and Garty H. (1997) *Am. J. Physiol.* **271**, 605-611
16. Debonneville, C., Flores, S.Y., Kamynina, E., Plant, P.J., Tauxe, C., Thomas, M.A., Munster C., Chraibi, A., Pratt, J.H., Horisberger, J.D., Pearce, D., Loffing, J., and Staub, O. (2001) *EMBO J* **20**, 7052-59

17. Snyder, P.M., Olson, D.R., and Thomas, B.C. (2002) *J Biol Chem* **277**, 5–8

18. Buck, T.M., Kolb, A.R., Boyd, C.R., Kleyman, T.R., and Brodsky, J.L. (2010) *Mol. Biol. Cell* **21**, 1047-1058
19. Lifton, R. P. (1995) *PNAS* **92**, 8545-8551
20. Nakamura, R. L. and Gaber, R. F. (1998) *Methods Enzymol* **293**, 89-104
21. Kashlan, O.B. and Kleyman, T.R. (2011) *Am J Physiol Renal Physiol* **301**, F684-F689
22. Garty, H. (1997) *Physiol. Rev.* **77**, 359-396
23. Bize, V., and Horisberger, J.D. (2007) *Am. J. Physiol. Renal Physiol.* **293**, 1137-1146
24. Sheng, S., Bruns, J.B., and Kleyman, T.R. (2004) *J. Biol. Chem.* **279**, 9743-9749
25. Collier, D.M., and Snyder, P.M. (2011) *J. Biol. Chem.* **286**, 6027-32
26. Collier, D.M., and Snyder, P.M. (2009) *J. Biol. Chem.* **284**, 792-798
27. Jasti, J. Furukawa, H., Gonzales, E.B., and Gouaux, E. (2007) *Nature* **449**, 316-322
28. Schild, L., Schneeberger, E., Gautschi, I., and Firsov, D. (1997) *J. Gen. Phys.* 109, 15-26
29. Gupta, S.S., and Canessa, C.M. (2000) *F.E.B.S. J.* **481**, 77-80
30. Wolfe, D.M., and Pearce, D.A. (2006) *NeuroMol. Med.* **8**, 279-306
31. Kolb, A.R., Buck, T.M., and Brodsky, J.L. (2011) *Am. J. Physiol. Renal Physiol.* **301**, F1-F11
32. Walker, G.M. (1998) *Yeast: Physiology and Biotechnology*. John Wiley & Sons Inc., New York, NY
33. Guthrie, C., and Fink, G., (2004) *Guide to Yeast Genetics and Molecular and Cell Biology*, Vol 194. Elsevier Academic Press, San Diego, California
34. Chraibi, A., and Horisberger, J.D. (2002) *Gen. Physiol.* **120**, 133-145
35. Carattino, M.D., Passero, C.J., Steren, C.A., Maarouf, A.B., Pilewski, J.M., Myerburg, M.M. Hughey, R.P. Kleyman, T.R. (2008) *Am. J. Physiol. Renal Physiol.* **294**, 47-52
36. Brown, T.L., LeMay, H.E., Bursten, B.E., and Murphy, C.J. (2009) *Chemistry: the central science*, 11Ed. Pearson Education, Inc, Upper Saddle River, NJ

VITA

Samantha Swann was born in Grand Prairie, TX on July 14, 1985 to Marsha Douget and Alan Swann. She grew up in the Houston area and ultimately graduated from Spring High School in 2003. Samantha attended Texas State University where she acquired a Bachelor's of Science in Clinical Laboratory Science and a Bachelors of Arts in Spanish in the fall of 2009. During her academic career, she was employed as a diamontologist working for Samuel's diamonds. In completion of her Spanish degree, she spent 6 months in Granada, Spain studying the Spanish language and culture. The following fall, Samantha was accepted into the Biochemsitry Graduate Program at Texas State under the direction of Dr. Rachell Booth.

Permanent Address

14901 Foy Drive

Austin, TX 78734

This thesis was typed by Samantha Swann